Summary of our JWST IDS GTO Program: Faint Object Time-Domain and (Pop III) Caustic Transits

Rogier Windhorst (ASU) — JWST Interdisciplinary Scientist

GTO team: T. Ashcraft, S. Cohen, R. Jansen, V. Jones, B. Joshi, D. Kim, B. Smith, F. Timmes, C. White (ASU), M. Alpaslan (NYU), D. Coe, N. Grogin, N. Hathi, A. Koekemoer, N. Pirzkal, A. Riess, R. Ryan, L. Strolger (STScI), C. Conselice, I. Smail (UK), W. Brisken, J. Condon, W. Cotton, K. Kellermann, R. Perley (NRAO), J. Diego, T. Broadhurst, (Spain), S. Driver, R. Livermore, M. Marshall, A. Robotham, S. Wyithe (OZ), K. Duncan, H. Rottgering (Leiden), S. Finkelstein, R. Larson (UT), G. Fazio, M Ashby, P. Maksym (CfA), B. Frye, M. Rieke, C. Willmer (UofA), H. Hammel (AURA), G. Hasinger (ESA), A. Kashlinsky, S. Milam, A. Straughn (GSFC), W. Keel (U-AL), P. Kelly (U-MN), P. S. Rodney (U-SC), M. Rutkowski (MNSU), H. Yan (U-MO), A. Zitrin (Israel).

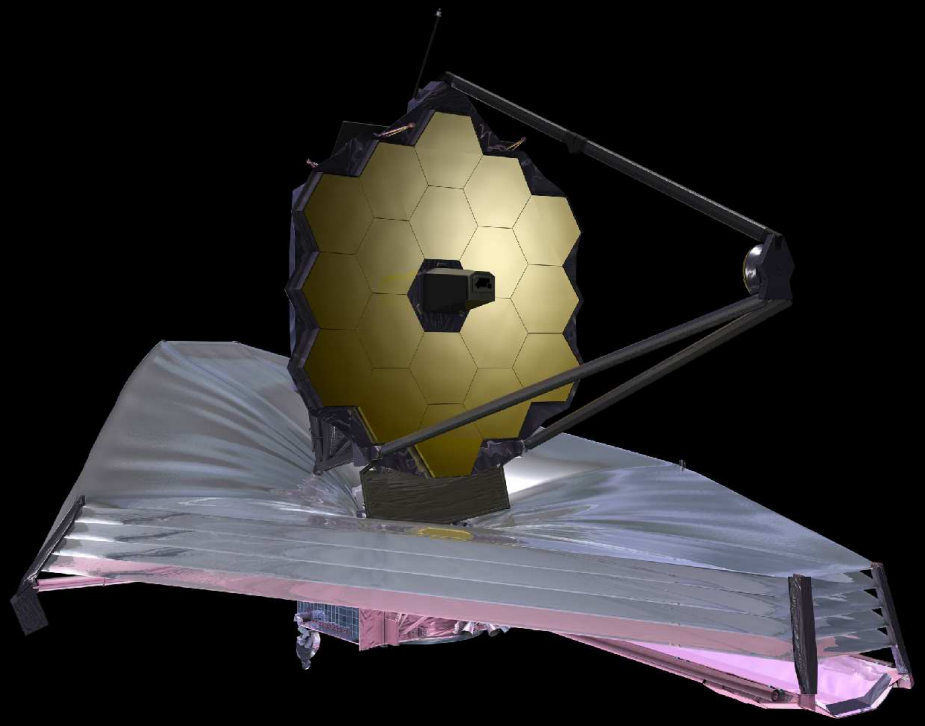

- Today, the JWST science remains as compelling as it was ∼20 years ago.
- In fact, the JWST science is far more exciting today than we could have imagined or planned for ∼20 years ago.

Talk at the JWST Science Working Group Telecon — Oct. 1, 2018

Talk is on: `http://www.asu.edu/clas/hst/www/jwst/jwsttalks/jwst_IDSGTOpgm_SWG_01oct18.pdf`

Outline & Conclusions

(1) JWST CVZ at the North (NEP) & South Ecliptic Pole (SEP).

(2) NIRCam + NIRISS-parallels can optimally cover the best NEP field.

(3) Unique new JWST Time-Domain Field (TDF) science in the NEP CVZ:

- Parallaxes (Extreme scattered KBO's, Comet nuclei at high Ecl. Lat?);
- Proper Motions (Brown Dwarfs: Galactic structure, atmos variability);
- Weak AGN Variability ($e.g.$, SF–AGN connection; support LyC studies);
- Very high redshift supernovae incl Pair Instability Supernovae (PISN).
- Dark sky in NEP TDF: CIB-fluctuations constrain First Light sources.

- The best area in the JWST NEP CVZ will be a Community Field for Time Domain science over 5–14 years (max JWST propellant life): first JWST epoch public rightaway + data products ASAP.

(4) In the best lensing clusters, possible JWST caustic transit detections of Pop III stars and their stellar-mass black hole accretion disks at $z \gtrsim 7$.

(1) JWST Continuous Viewing Zones (CVZs): North & South Ecliptic Poles.

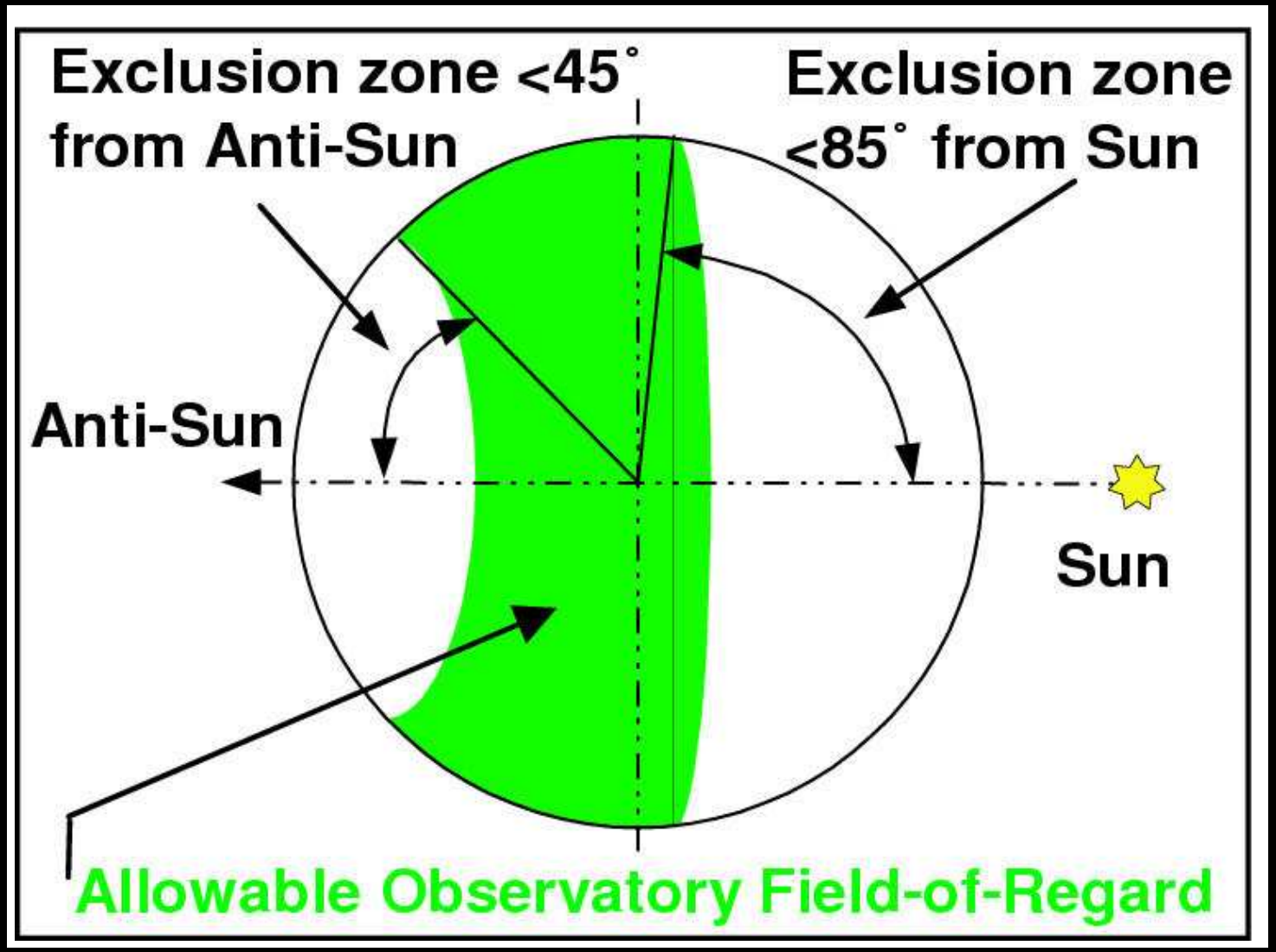

Accessible by JWST 365 days/yr: *only* the NEP & SEP CVZ (r $\lesssim 5^{\circ}$):

- NEP has great regions for far-extragalactic science. SEP contains LMC.
- CVZs great for parallax, proper motions, high redshift variability, etc.
- JWST NEP survey also provides multi-ORIENT grism spectral separation.

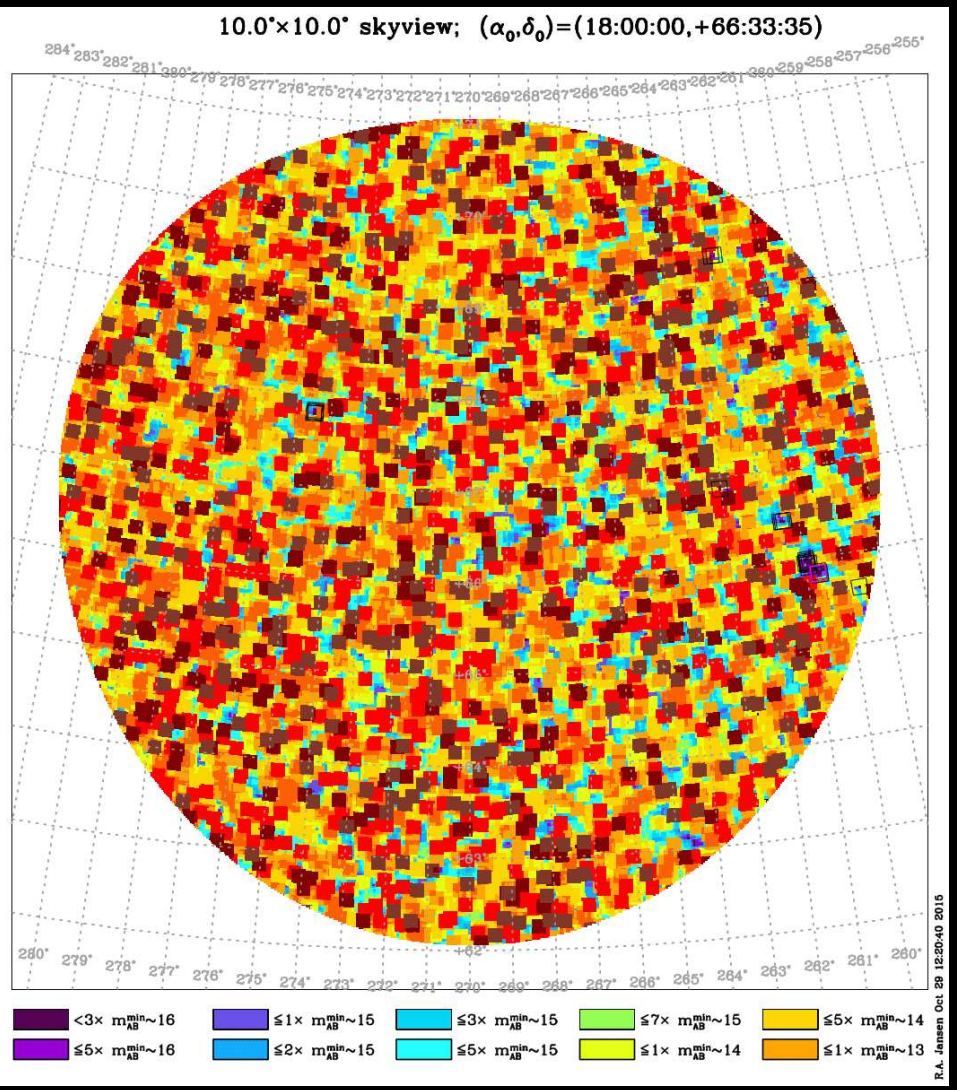

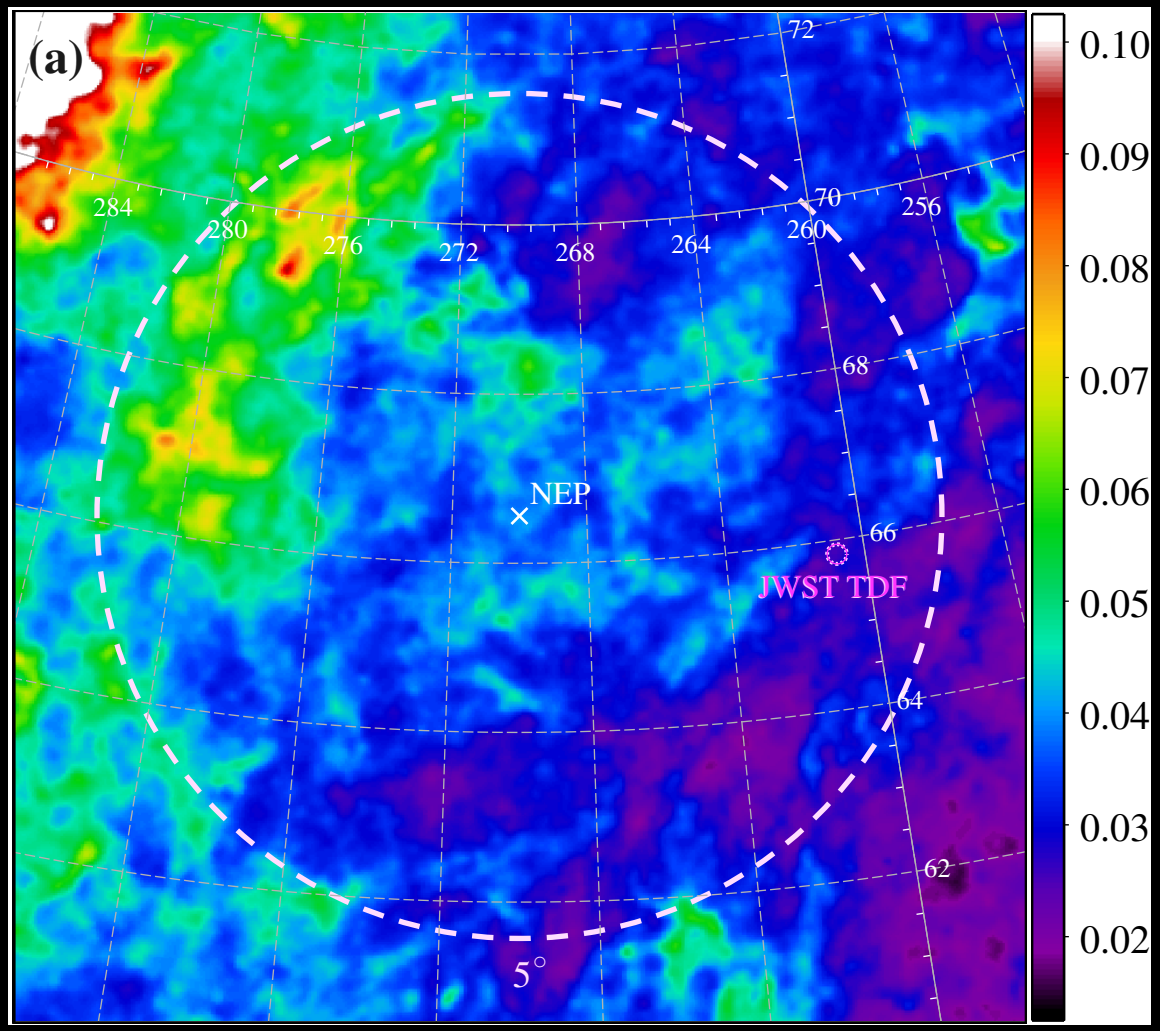

[LEFT]: *WISE* 4μm bright-object penalties in 10′ boxes: Very few regions (purple) exist *without bright stars* (AB$\lesssim$16 mag), needed to minimize persistence in JWST images (Jansen & Windhorst, astro-ph/1807.05278v2).

[RIGHT]: *E(B−V)* map (Schlegel$^+$ 1998) in same NEP-region ($b^{II} \simeq 33°$). Cleanest r=7′ region for JWST has modest extinction: $E(B-V) \lesssim 0.028^m$.

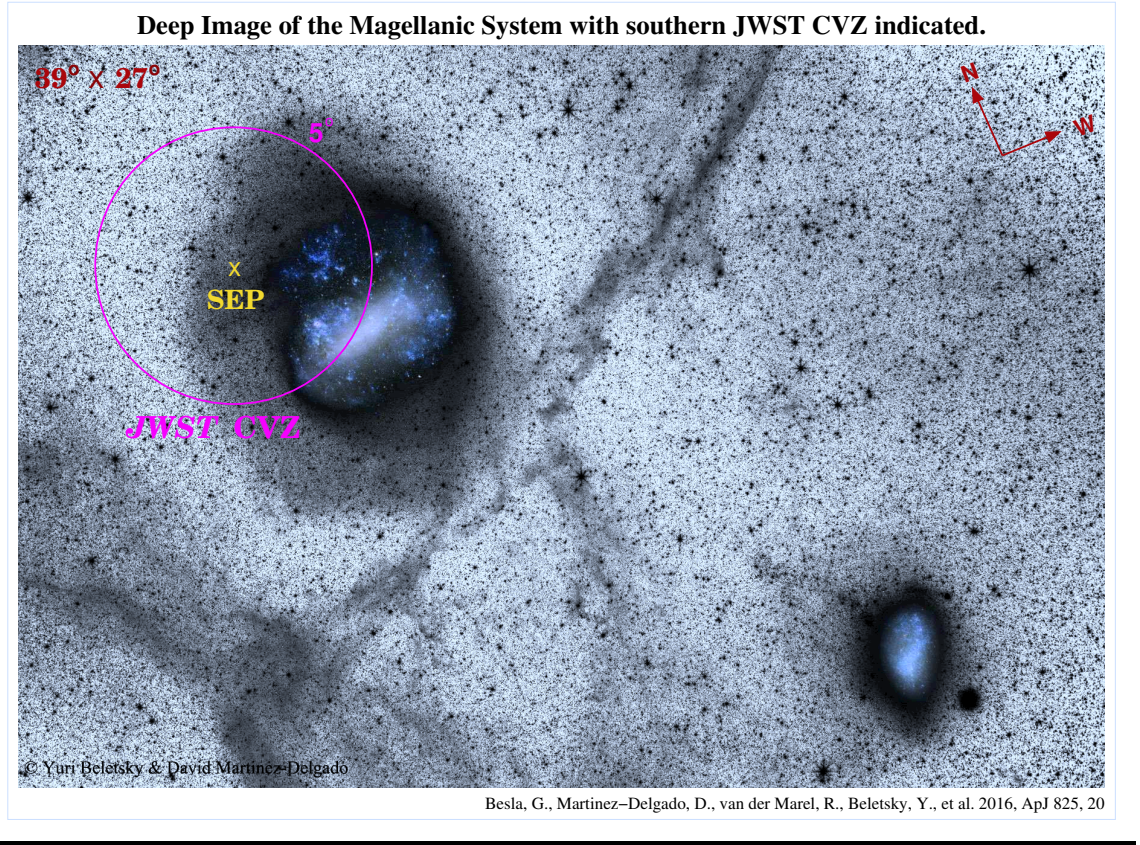

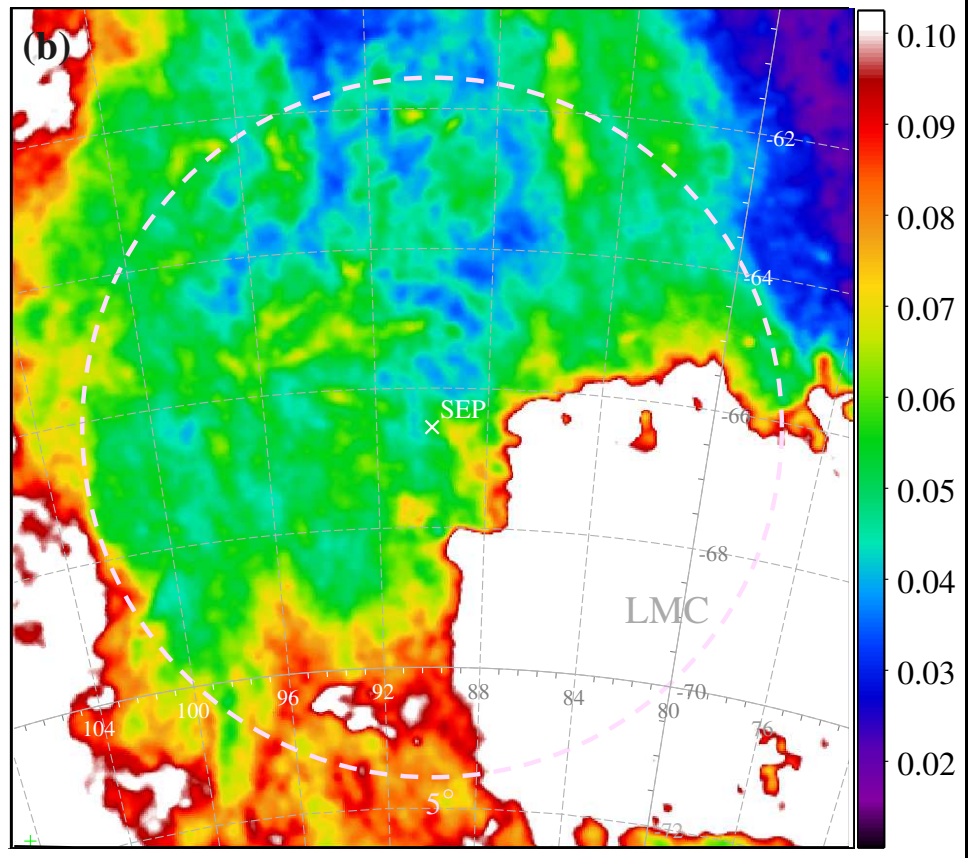

[LEFT] Map of LMC+SMC and spurs (Besla et al. 2016, ApJ, 825, 20).

[RIGHT]: *E(B−V)* map (Schlegel et al. 1998) in SEP-region.

- SEP will be good for CVZ studies of LMC and its outskirts.
- SEP/LMC can serve as counter-target for NEP surveys: offsets accumulated angular momentum, and so help save JWST propellant/lifetime.
- JWST should observe and monitor bottom of IMF in LMC at SEP.

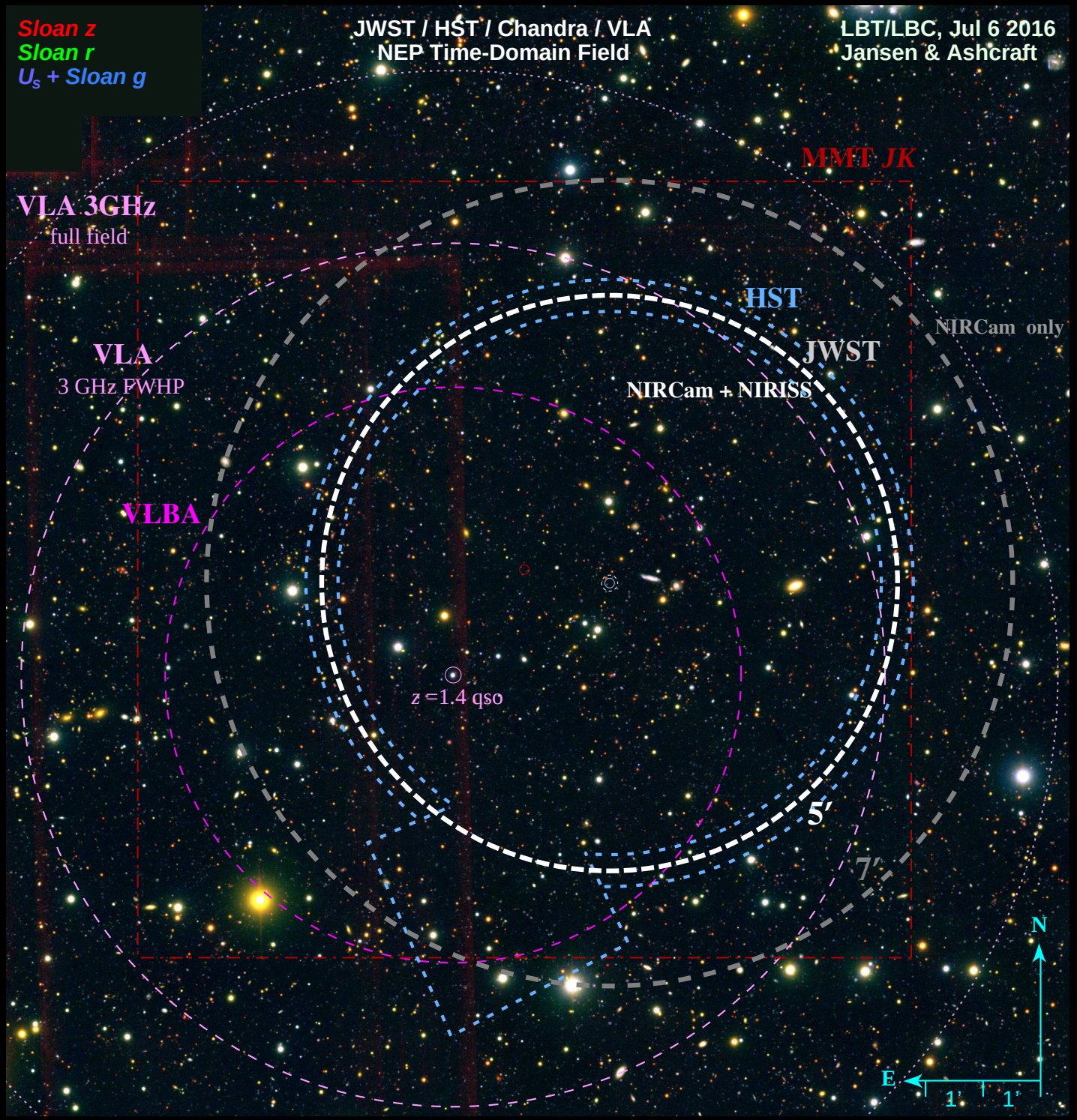

Intended r=7′ JWST NEP TDF is indeed free of bright (AB≲16) stars.

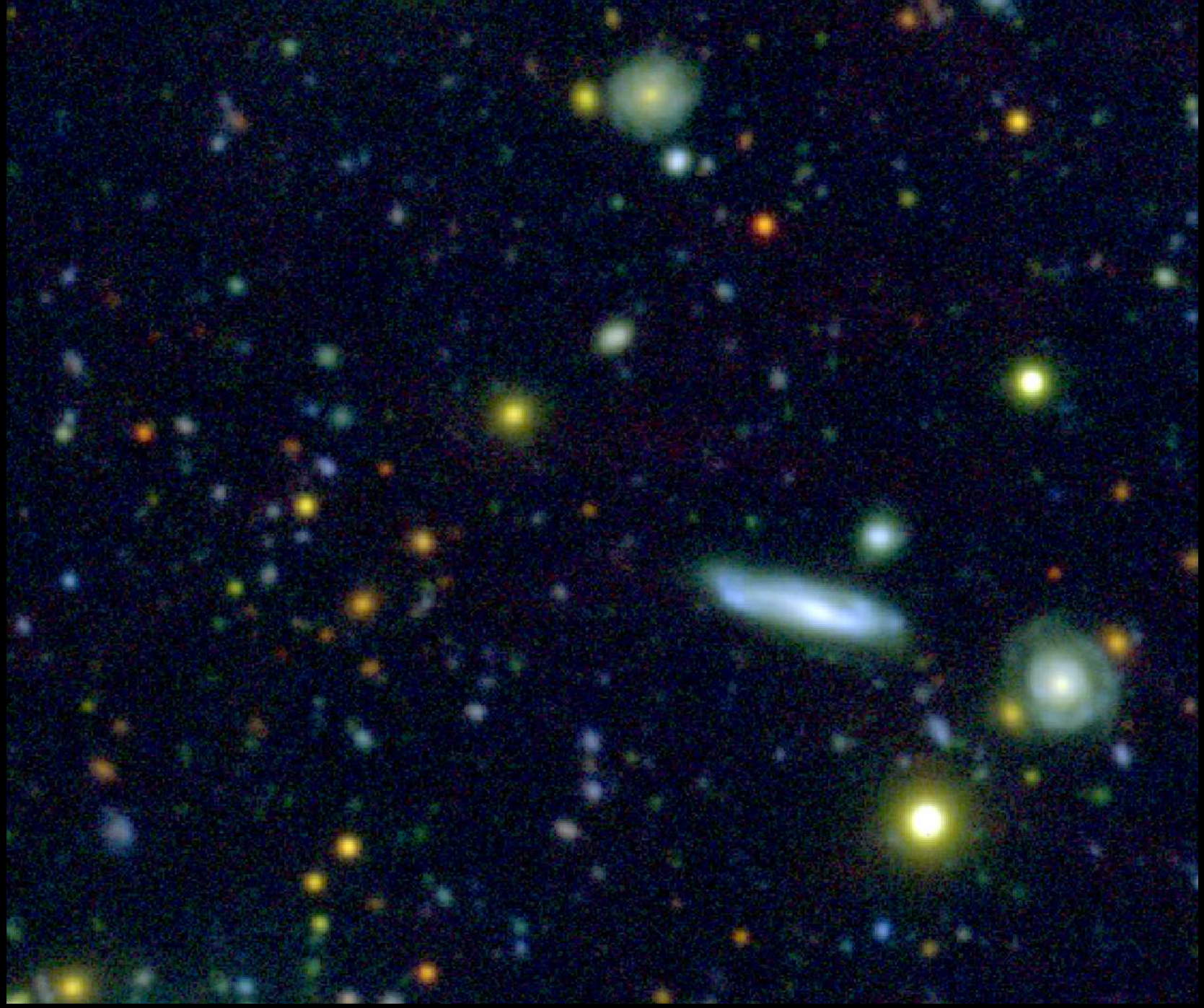

At r$\lesssim$7′, JWST NEP TDF is a normal clean extragalactic survey field.

To AB$\lesssim$26 mag, get many faint Galactic brown dwarfs and high-z dropouts.

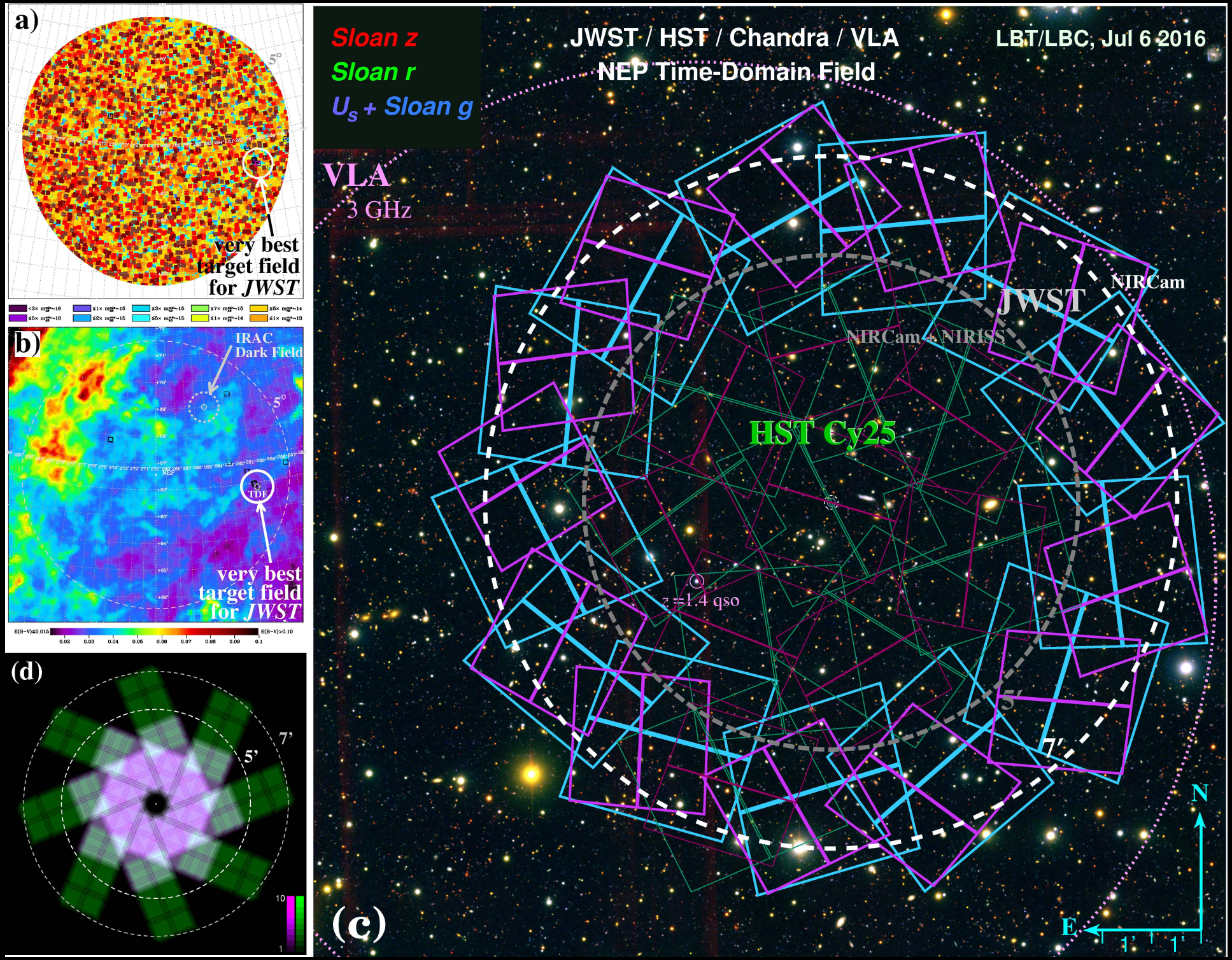

- r=7′ JWST NEP TDF with HST Cy≳25 ACS+WFC3 mosaics overlaid.

(2) NIRCam + NIRISS-parallels optimally cover the best NEP TDF.

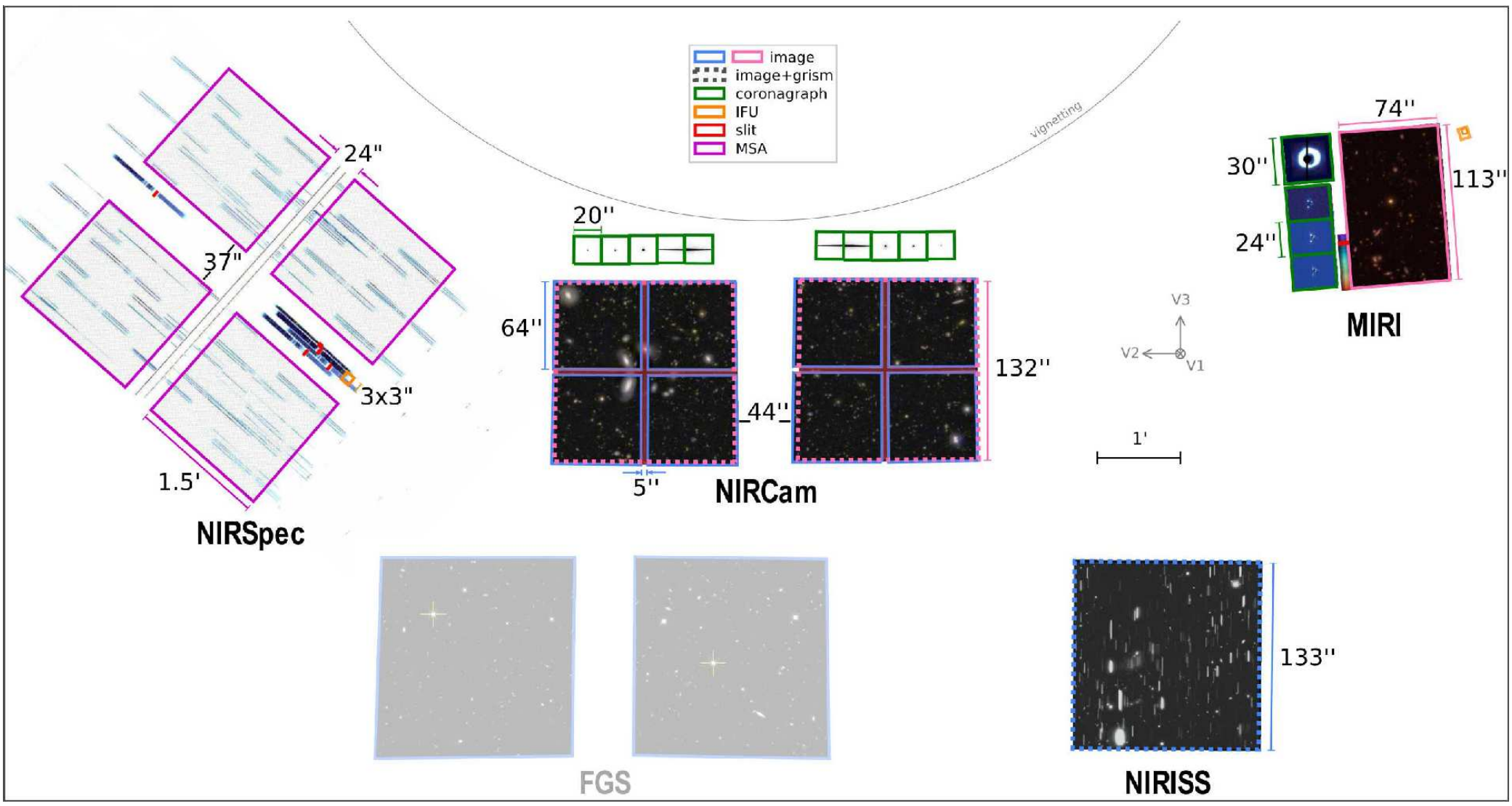

- FY$\gtrsim$16: most-used JWST instrument pairs implemented for science parallels.
- CVZ enables well-overlapping *dark-sky* NIRCam + NIRISS-parallel mosaics.
  - JWST NIRISS (or NIRCam LW) parallel grism science is essential!

Exposure Maps of NEP JWST-Windmill & GO-Extensions:

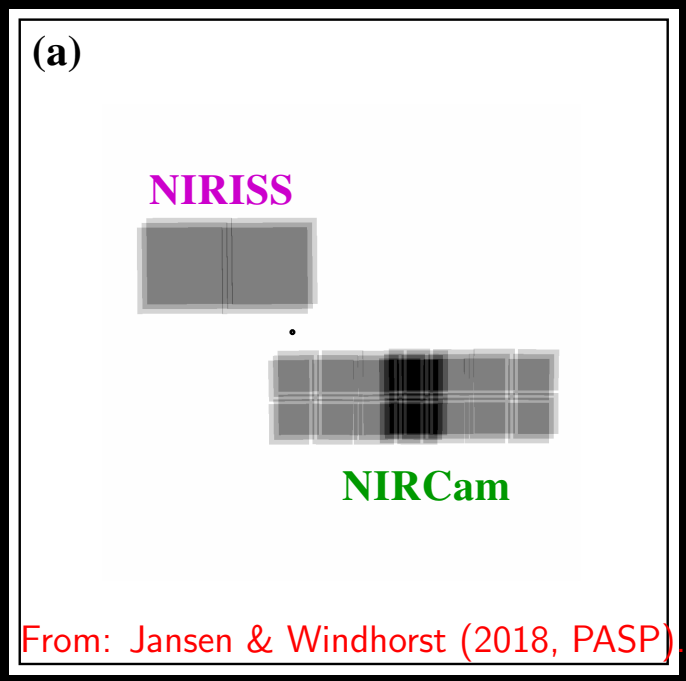

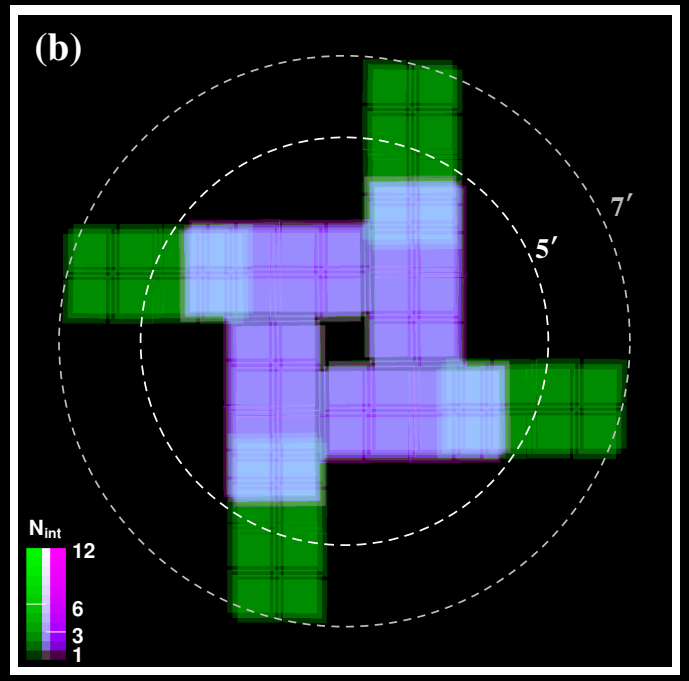

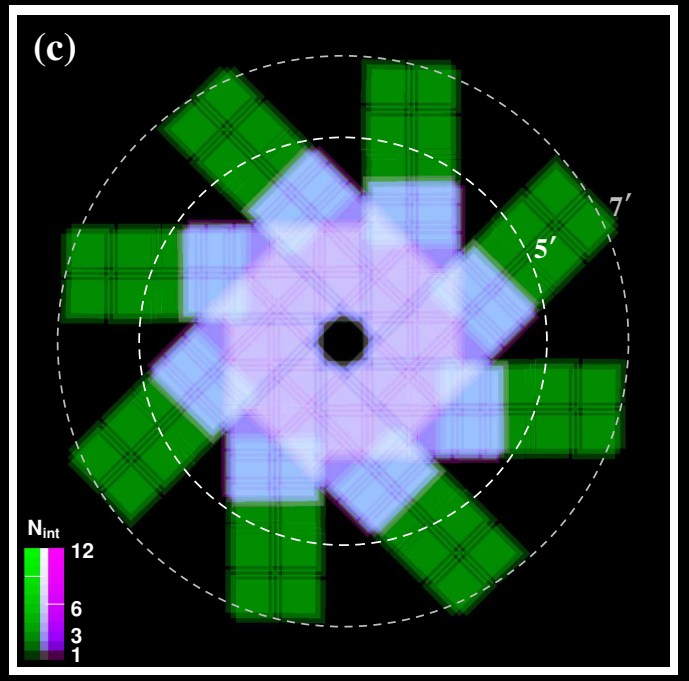

[LEFT]: Exposure map ($15' \times 15'$) of two offset contiguous areas: NIRCam primary (green) + NIRISS parallel grism (purple), observable at ΔPA=any$^\circ$.

[MIDDLE]: Same with ΔPA=90+180+270° added: our 50-hr GTO plan.

[RIGHT]: Possible 8-epoch GO-Community extension in JWST Cycle $\gtrsim$1.

Lighter regions: NIRCam exposures overlap, reaching $\sim$0.75 mag deeper.

NEP 2.0μm sky *always* dark: 0.24$\pm$0.03 MJy/sr. GOODS$\sim$0.19–0.35/0.5 yr.

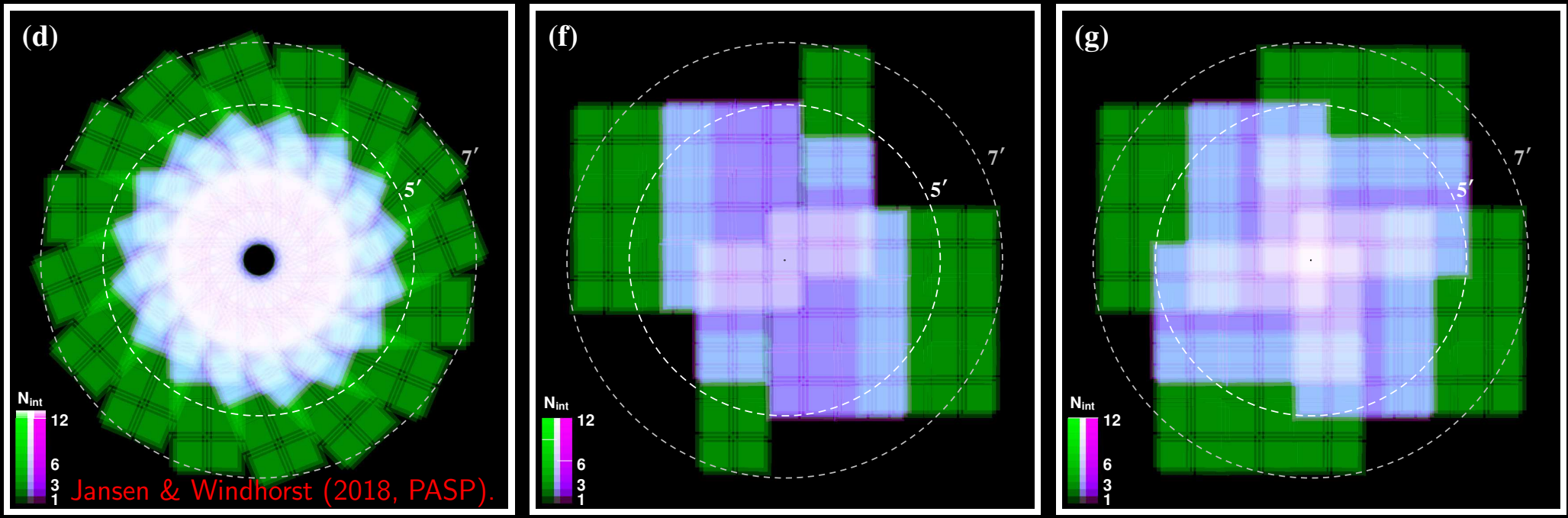

[LEFT]: Example of 16-epoch extension. Alternatively:

[MIDDLE]: 4-epoch filled NIRCam + NIRISS Windmill mosaic.

[RIGHT]: 4-epoch extended NIRCam + NIRISS Windmill mosaic.

- GO's can repeat NIRCam primaries + NIRISS parallels as often as needed during JWST's 5–14 year lifetime at any PA — no ORIENT restrictions!

- NEP yields time-domain imaging to AB$\lesssim$29 (after WFE-drift correction!).
- NEP provides robust multi-ORIENT grism spectra to AB$\lesssim$28 mag.

(3) JWST Proper-Motion Science possible in the NEP TDF:

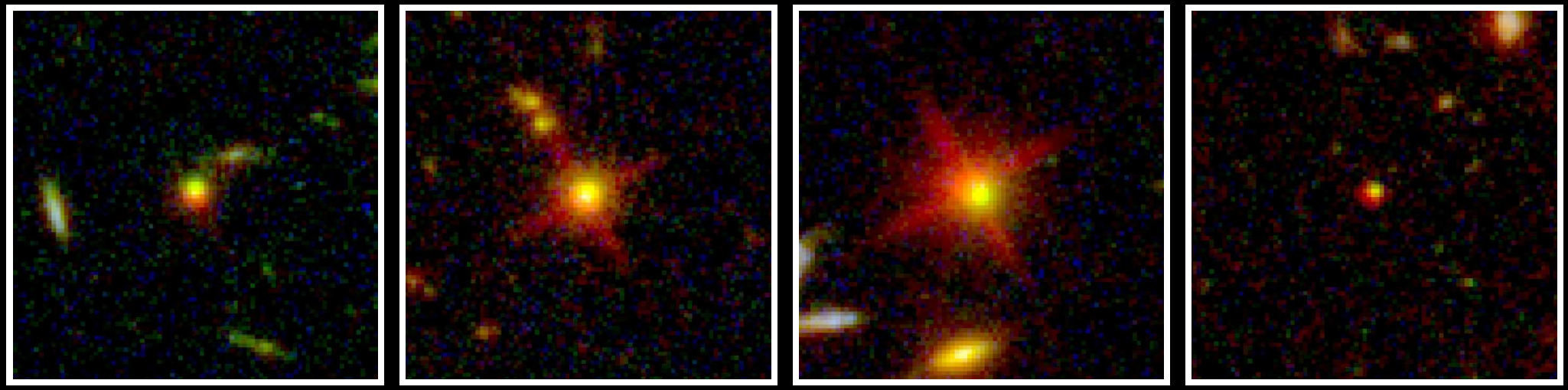

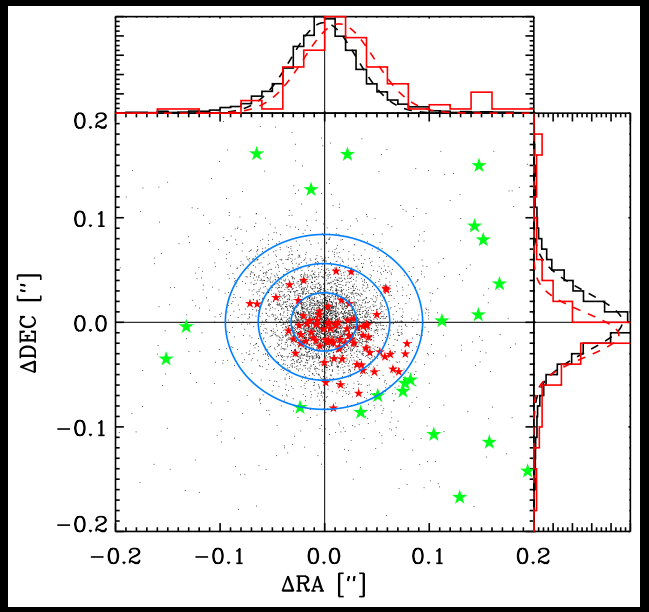

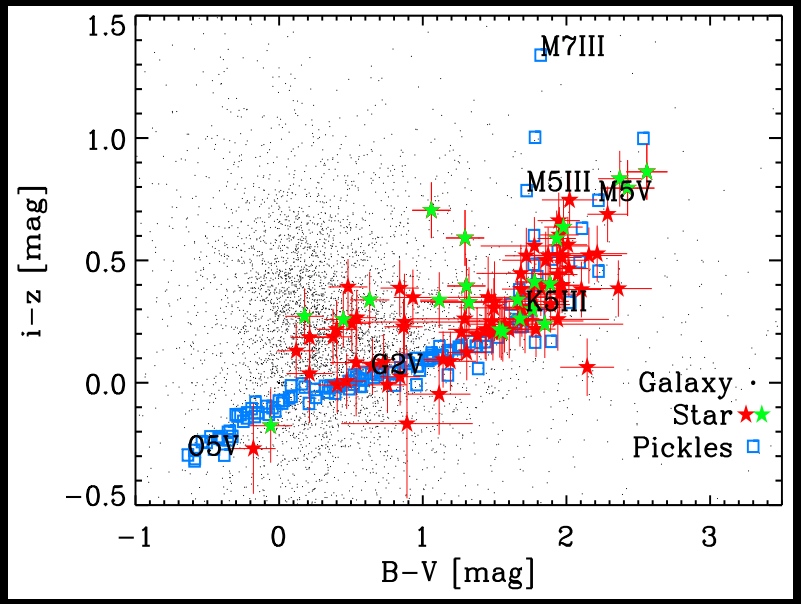

6-year WFC3-ACS high Proper-Motion (PM) stars in the WFC3 ERS (W11):

PM$\simeq$3.06 m.a.s./yr (4.6σ; AB$\lesssim$27), constraining Galactic structure models.

JWST (+Gaia/VLBA) yields m.a.s. PM to AB$\lesssim$29 mag in $\lesssim$2 yrs.

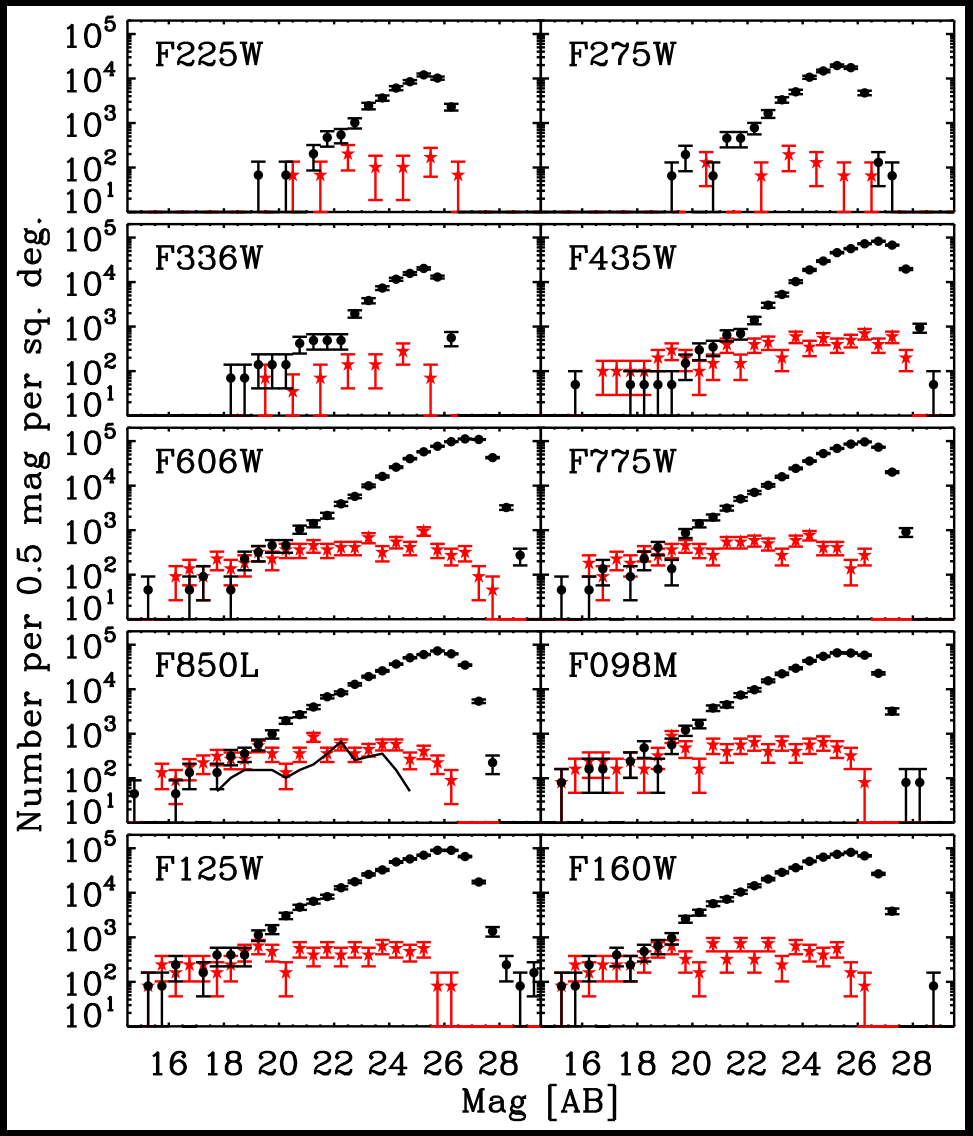

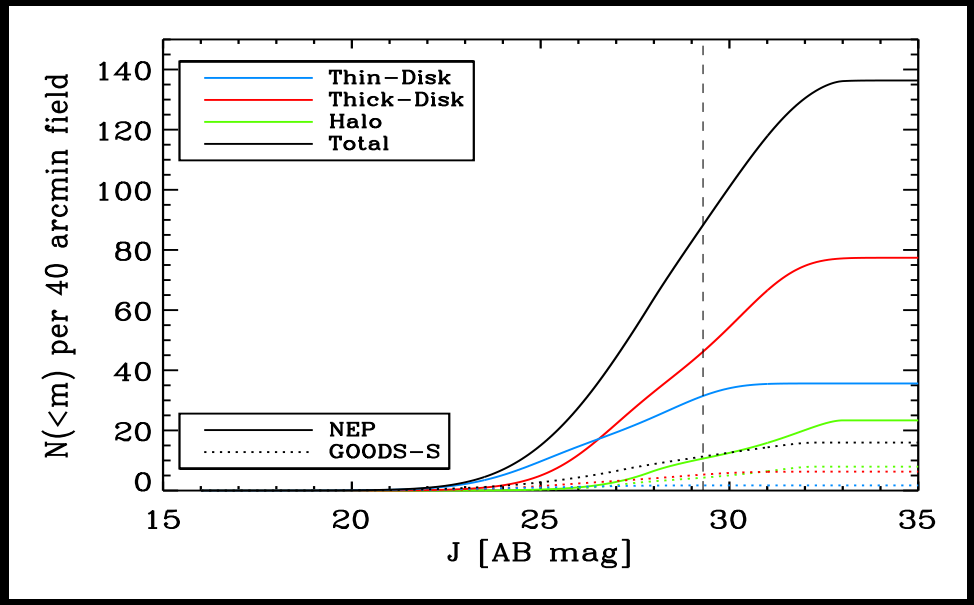

From WFC3/ERS (Windhorst et al. 2011; W11):

[LEFT] Panchromatic galaxy counts vs. star-counts in WFC3 ERS.

Galaxy count slope steeper than stars, so gals outnumber stars at AB$\gtrsim$21.

[RIGHT] Ryan & Reid (2015) model: 6–9$\times$ more brown dwarfs in NEP.

JWST NEP will have $\lesssim 10^{-5}$–10^{-4} of pixels covered by stars to AB$\lesssim$29.

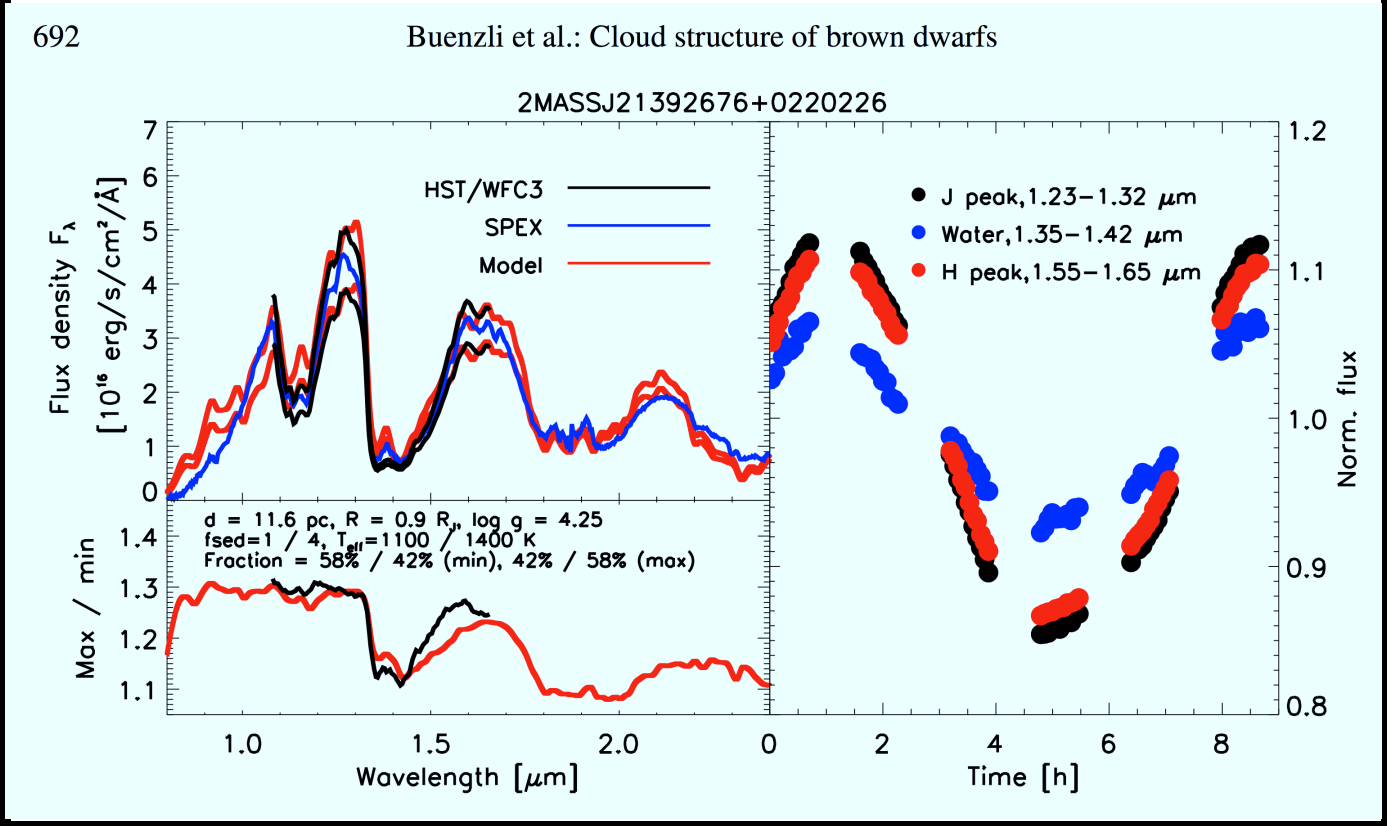

[Top]: Varying HST/WFC3 spectrum (black) compared to average brown dwarf spectrum (blue; Burgasser et al. 2014 SPEX library).

Red overplots the best patchy cloud model of Buenzli et al. (2014).

[Bottom]: Max/Min ratio of data (black) & model (red) for indicated physical parameters; [Right]: Measured broad-band light curves over 6 orbits.

- JWST NEP TDF can monitor $\sim$100 faint BDs to AB$\lesssim$29 mag.
- Hours-weeks timescales will constrain rotation curves & cloud coverage.
- VLA μJy: chromospheric/coronal magnetic activity $\longrightarrow$ BD-like/auroral?

(3) Unique new JWST Variability Science possible in the NEP TDF:

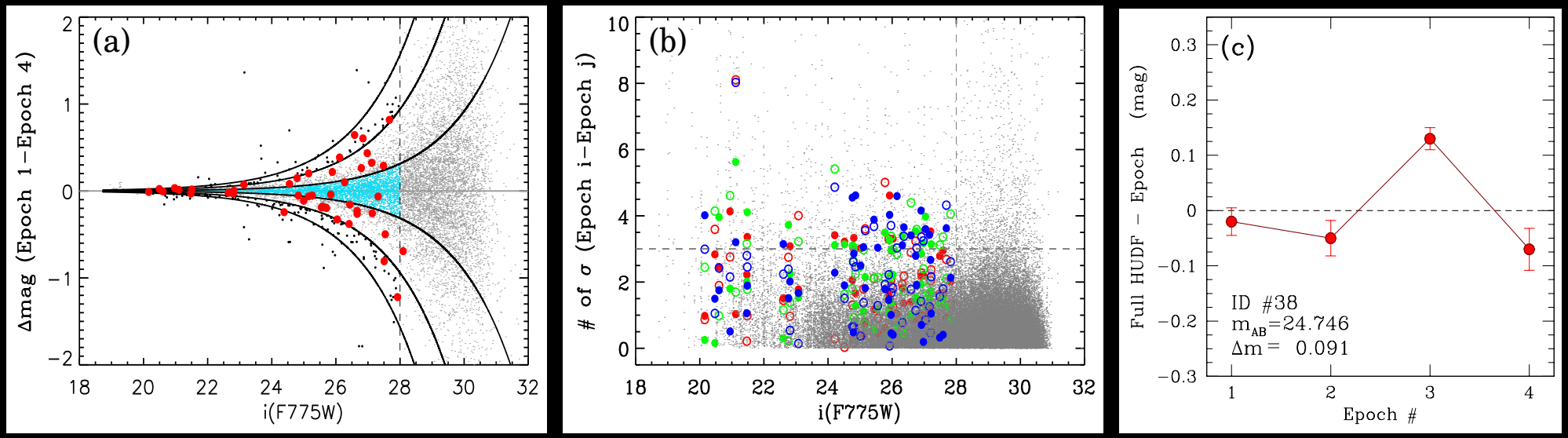

[LEFT] Flux diff. between 2 HUDF epochs vs. i-mag (Cohen et al. 2006).

- Red points mark $\gtrsim 3\sigma$ variables between 6 epoch pairs to AB$\lesssim$28 mag.

[MIDDLE] All-epoch flux differences in σ; [RIGHT] Weak AGN point-source with 20% flux variation on months timescales ($\simeq$restframe weeks).

- Need JWST resolution to detect embedded AGN variability (or SNe).
- JWST NEP may show a few % of all objects to have variable weak AGN on timescales of months–years to AB$\lesssim$29–30 mag.
- JWST NEP will provide a *robust, independent* way to select weak AGN, complementing NIRCam colors + NIRISS grism emission lines.
- Plus 6-epoch Chandra and 10-epoch VLA+VLBA μJy images, etc.

(3) Galaxy & Variable Weak AGN Contributions to Escaping LyC:

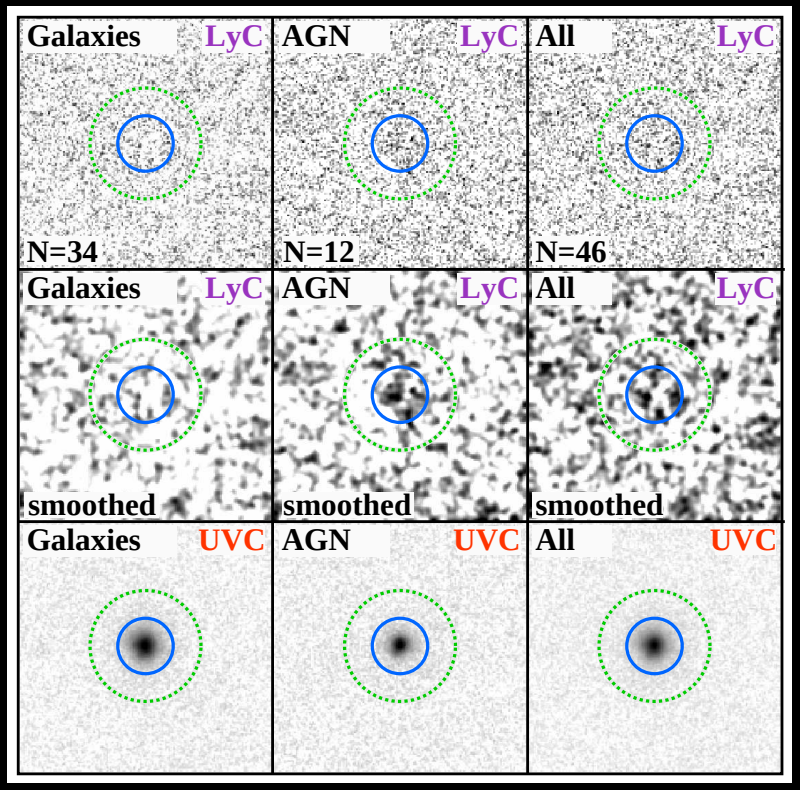

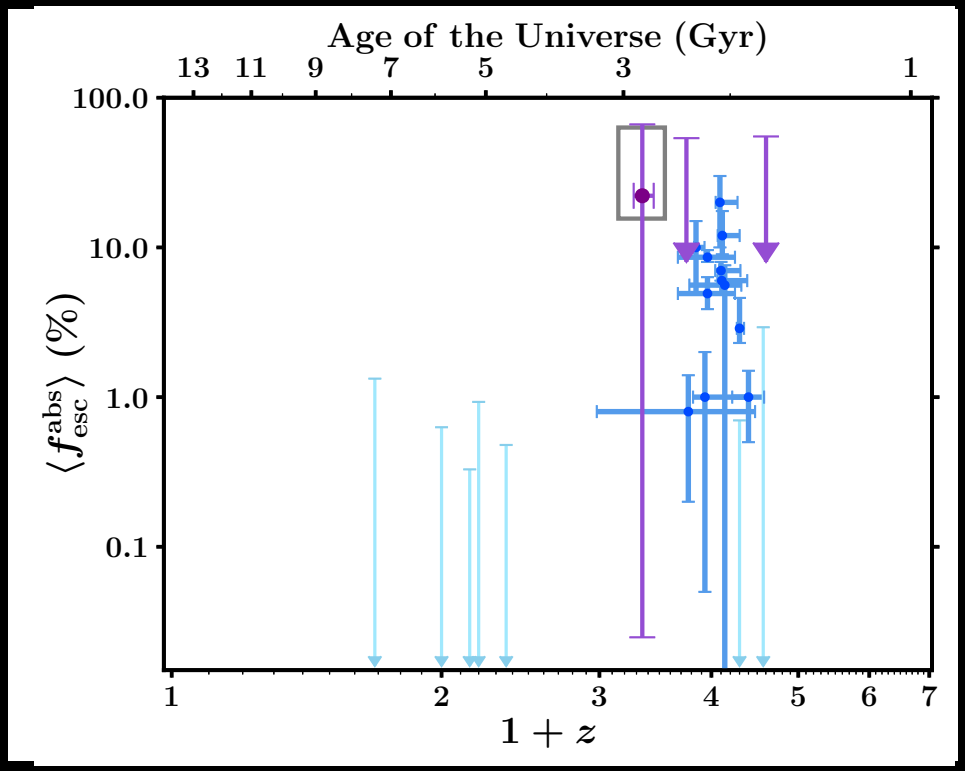

[LEFT] WFC3/ERS galaxies & weak AGN in UV (Smith+; 2018, ApJ, 853, 191):

Left-to-Right: Galaxies w/o AGN, Weak AGN, All Objects; Top-to-Bottom: LyC, LyC-smoothed, UV-continuum.

- Stacked WFC3 LyC emission has a *very flat* SB-distribution with radius.

[RIGHT] Absolute f_{esc} of galaxies increases with redshift.

- Galaxies may dominate/complete reionization at $3 \lesssim z \lesssim 6$, while
- Weak AGN may dominate and maintain reionization at $z \lesssim 3$.
- NIRISS provides $\gtrsim$500 z's to AB$\lesssim$28, 10-folding LyC statistics in NEP.

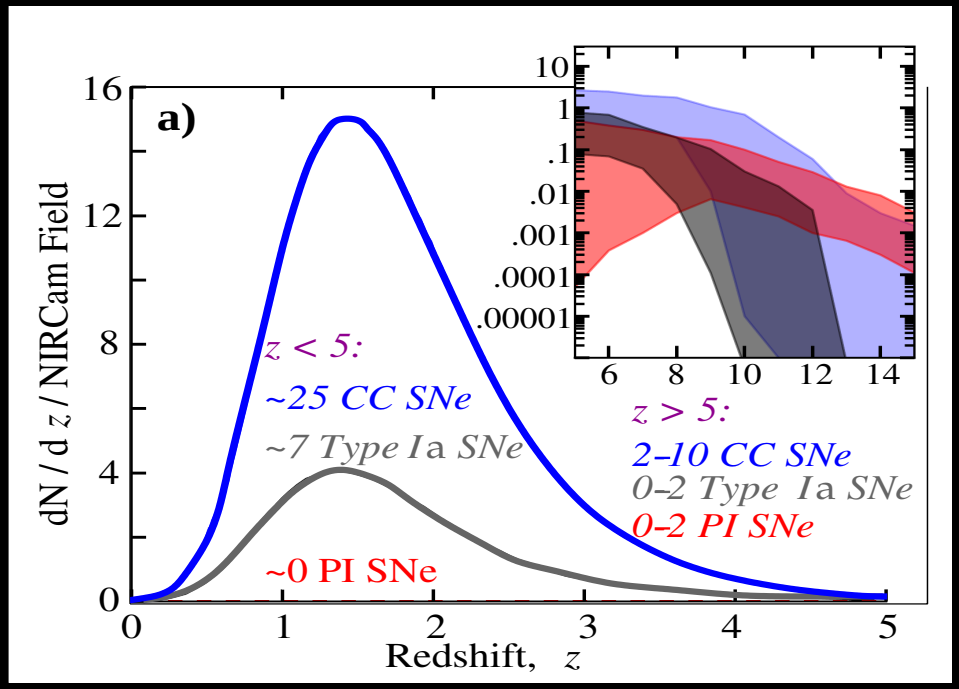

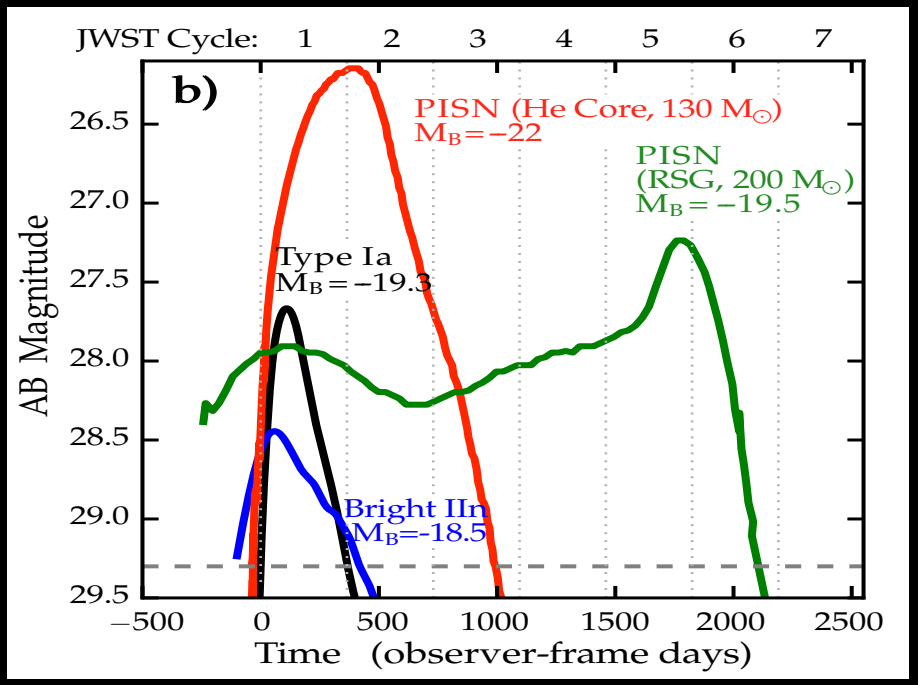

[LEFT] Projected Supernova yield for a single JWST/NIRCam field: r$\sim 7'$ JWST NEP TDF provides $\sim$16$\times$ more high-z SNe than 1 NIRCam.

- JWST NEP will detect *every* Type Ia SN to z$\lesssim$5, and 90% of all Core Collapse (CC) SNe to z$\lesssim$1.5 (Rodney et al. 2015; Strolger et al. 2015).

[RIGHT] Simulated light curves for various SN types at z=7. JWST may detect some (rare) Pair Instability SuperNovae (PISN; Kasen et al. 2011).

- 7-yr timescale of massive PISN: Must start NEP field in JWST Cycle 1.
- The JWST NEP Time-Domain field is critical for high-z SN work:
- NEP can monitor SNe (+hosts) as often as needed, including SNe at z$\gtrsim$5.

(3) Other Science Enabled by the Always-Dark JWST NEP Sky:

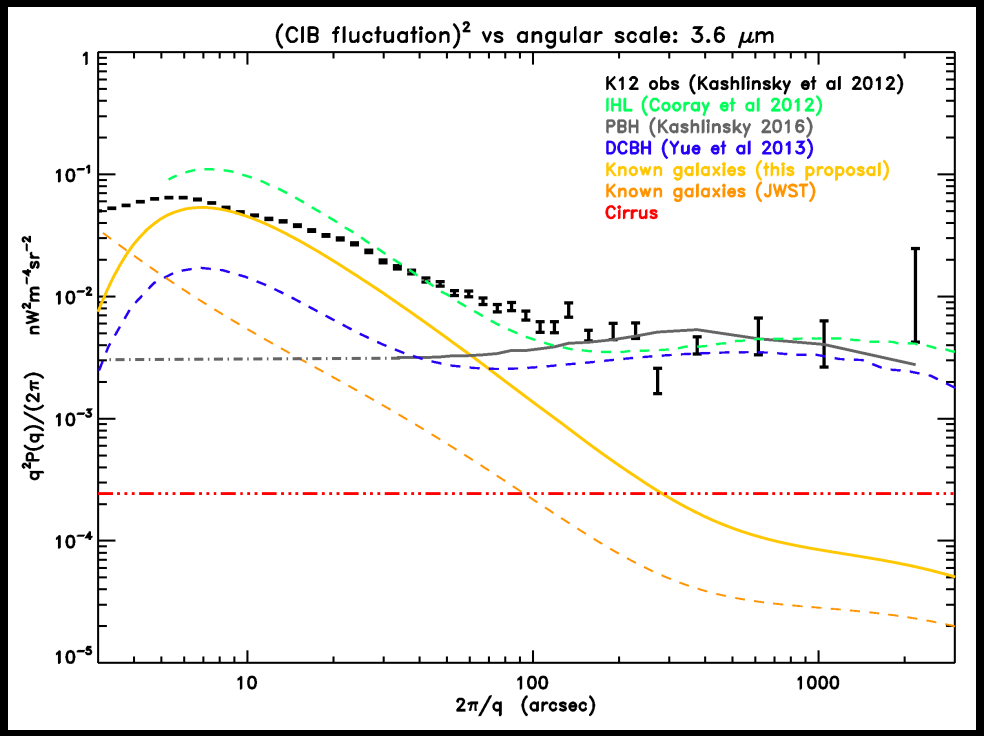

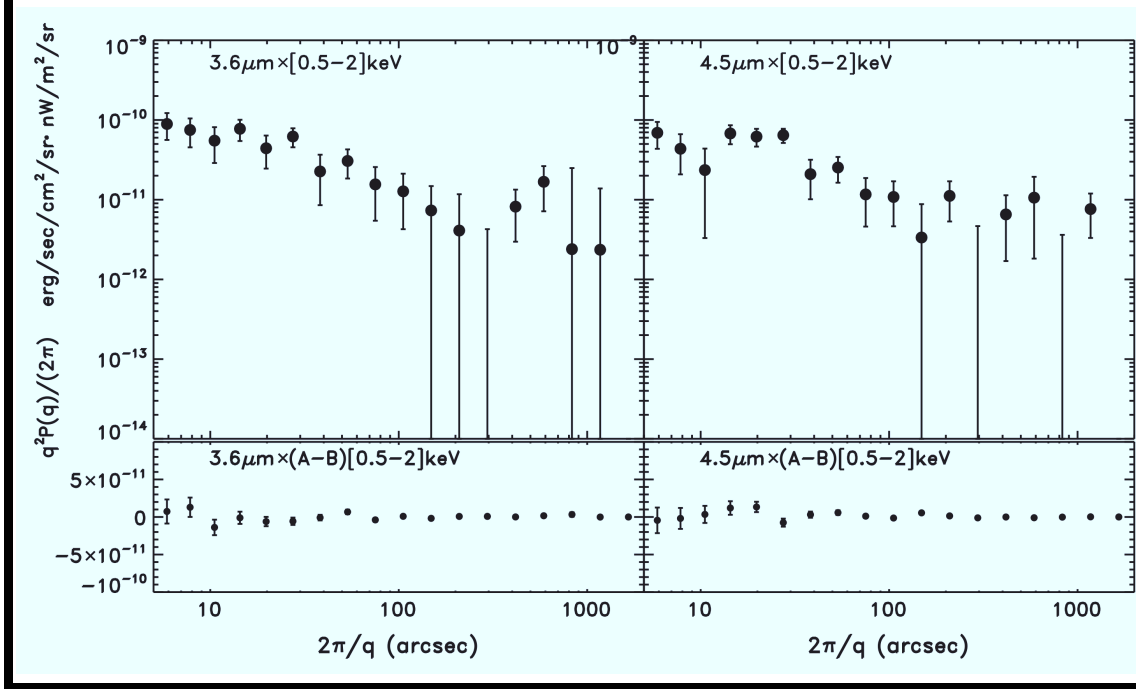

[LEFT] Object-free Spitzer 3.6 μm power-spectrum constrain CIB fluctuation models (Cappelluti et al. 2017; Kashlinsky et al. 2012, 2015, 2018):

- Orange dashes show ($\gtrsim$50 hr, $10\times10'$) JWST NEP CIB-limits, $e.g.$, : Primordial black hole models (PBHs; Kashlinsky et al. 2016); or Direct-collapse black hole models models (DCBHs; Yue et al. 2015).

[RIGHT] Spitzer–Chandra cross-corr spectrum (Mitchell-Wynne et al. 2016):

- Pop III objects at z$\gtrsim$7 have sky-SB $\gtrsim$31 mag/arcs^2, + likely a (stellar mass) black hole component (Kashlinsky$^+$ 2018, Windhorst$^+$ 2018).

(4) Possible caustic transits from Pop III stars and their BH accretion disks.

The Astrophysical Journal Supplement Series, 234:41 (40pp), 2018 February https://doi.org/10.3847/1538-4365/aaa760

CrossMark

On the Observability of Individual Population III Stars and Their Stellar-mass Black Hole Accretion Disks through Cluster Caustic Transits

Rogier A. Windhorst[1], F. X. Timmes[1], J. Stuart B. Wyithe[2], Mehmet Alpaslan[3], Stephen K. Andrews[4], Daniel Coe[5], Jose M. Diego[6], Mark Dijkstra[7], Simon P. Driver[4], Patrick L. Kelly[8], and Duho Kim[1]

[1] School of Earth and Space Exploration, Arizona State University, Tempe, AZ 85287-1404, USA; Rogier.Windhorst@asu.edu, Francis.Timmes@asu.edu
[2] University of Melbourne, Parkville, VIC 3010, Australia; SWyithe@physics.unimelb.edu.au
[3] New York University, Department of Physics, 726 Broadway, Room 1005, New York, NY 10003, USA
[4] The University of Western Australia, 35 Stirling Highway, Crawley, WA 6009, Australia
[5] Space Telescope Science Institute, 3700 San Martin Drive, Baltimore, MD 21218, USA
[6] IFCA, Instituto de Fisica de Cantabria (UC-CSIC), Avenida de Los Castros s/n, E-39005 Santander, Spain
[7] Institute of Theoretical Astrophysics, University of Oslo, NO-0315 Oslo, Norway
[8] University of California at Berkeley, Berkeley, CA 94720-3411, USA
Received 2017 November 22; revised 2018 January 6; accepted 2018 January 10; published 2018 February 14

Abstract

We summarize panchromatic Extragalactic Background Light data to place upper limits on the integrated near-infrared surface brightness (SB) that may come from Population III stars and possible accretion disks around their stellar-mass black holes (BHs) in the epoch of First Light, broadly taken from $z \simeq 7$–17. Theoretical predictions and recent near-infrared power spectra provide tighter constraints on their sky signal. We outline the physical properties of zero-metallicity Population III stars from MESA stellar evolution models through helium depletion and of BH accretion disks at $z \gtrsim 7$. We assume that second-generation non-zero-metallicity stars can form at higher multiplicity, so that BH accretion disks may be fed by Roche-lobe overflow from lower-mass companions. We use these near-infrared SB constraints to calculate the number of caustic transits behind lensing clusters that the *James Webb Space Telescope* and the next-generation ground-based telescopes may observe for both Population III stars and their BH accretion disks. Typical caustic magnifications can be $\mu \simeq 10^4$–10^5, with rise times of hours and decline times of $\lesssim$1 year for cluster transverse velocities of $v_T \lesssim 1000$ km s^{-1}. Microlensing by intracluster-medium objects can modify transit magnifications but lengthen visibility times. Depending on BH masses, accretion-disk radii, and feeding efficiencies, stellar-mass BH accretion-disk caustic transits could outnumber those from Population III stars. To observe Population III caustic transits directly may require monitoring 3–30 lensing clusters to AB $\lesssim$ 29 mag over a decade.

Key words: accretion, accretion disks – galaxies: clusters: general – gravitational lensing: strong – infrared: diffuse background – stars: black holes – stars: Population III

Windhorst$^+$ (2018, ApJS, 234, 41): JWST (and 25–39 m ground-based telescopes?) may detect Pop III stars and their stellar-mass BH accretion disks *directly* to AB$\lesssim$28–29 mag via caustic transits in the right clusters.

- JWST GO community should anticipate this and build on it.

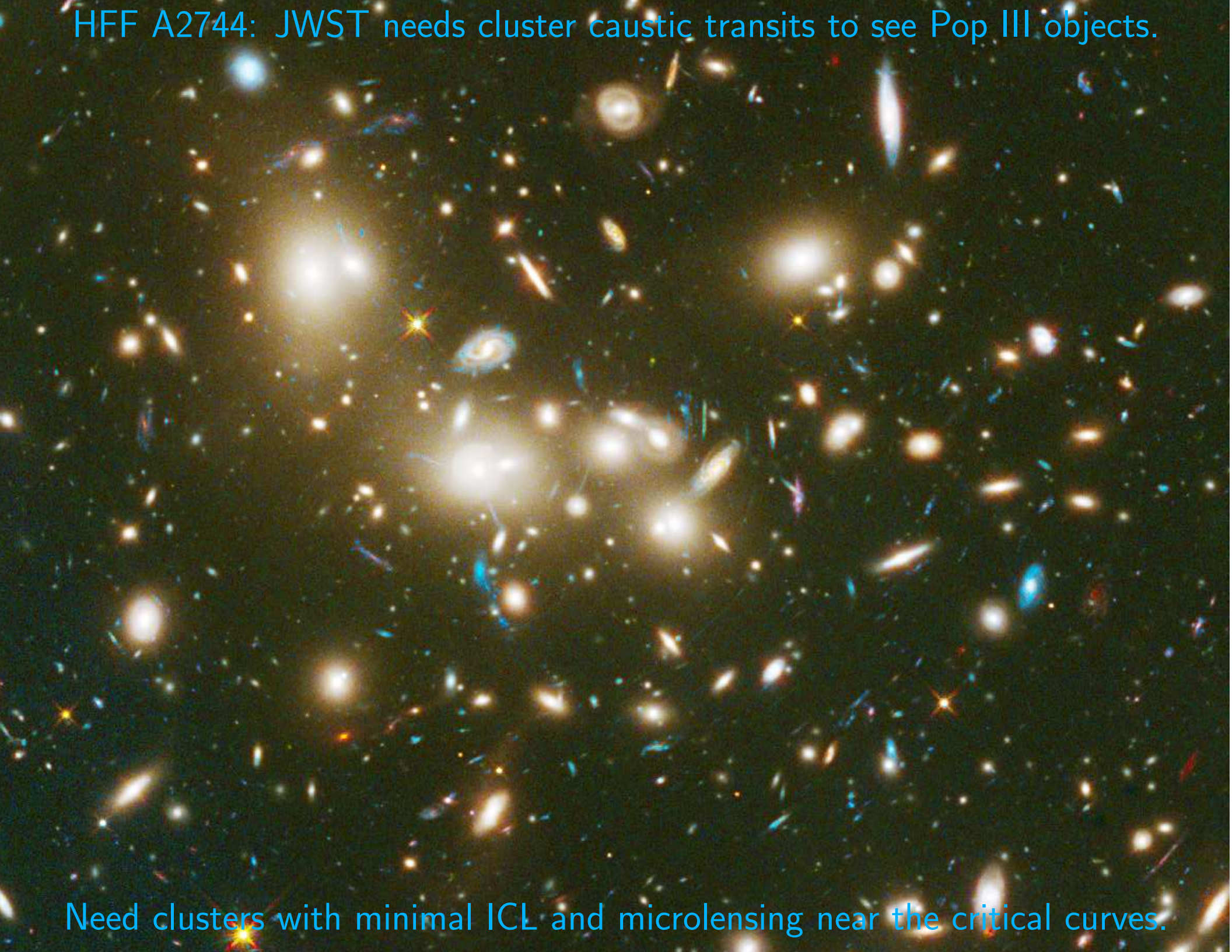
HFF A2744: JWST needs cluster caustic transits to see Pop III objects.
Need clusters with minimal ICL and microlensing near the critical curves.

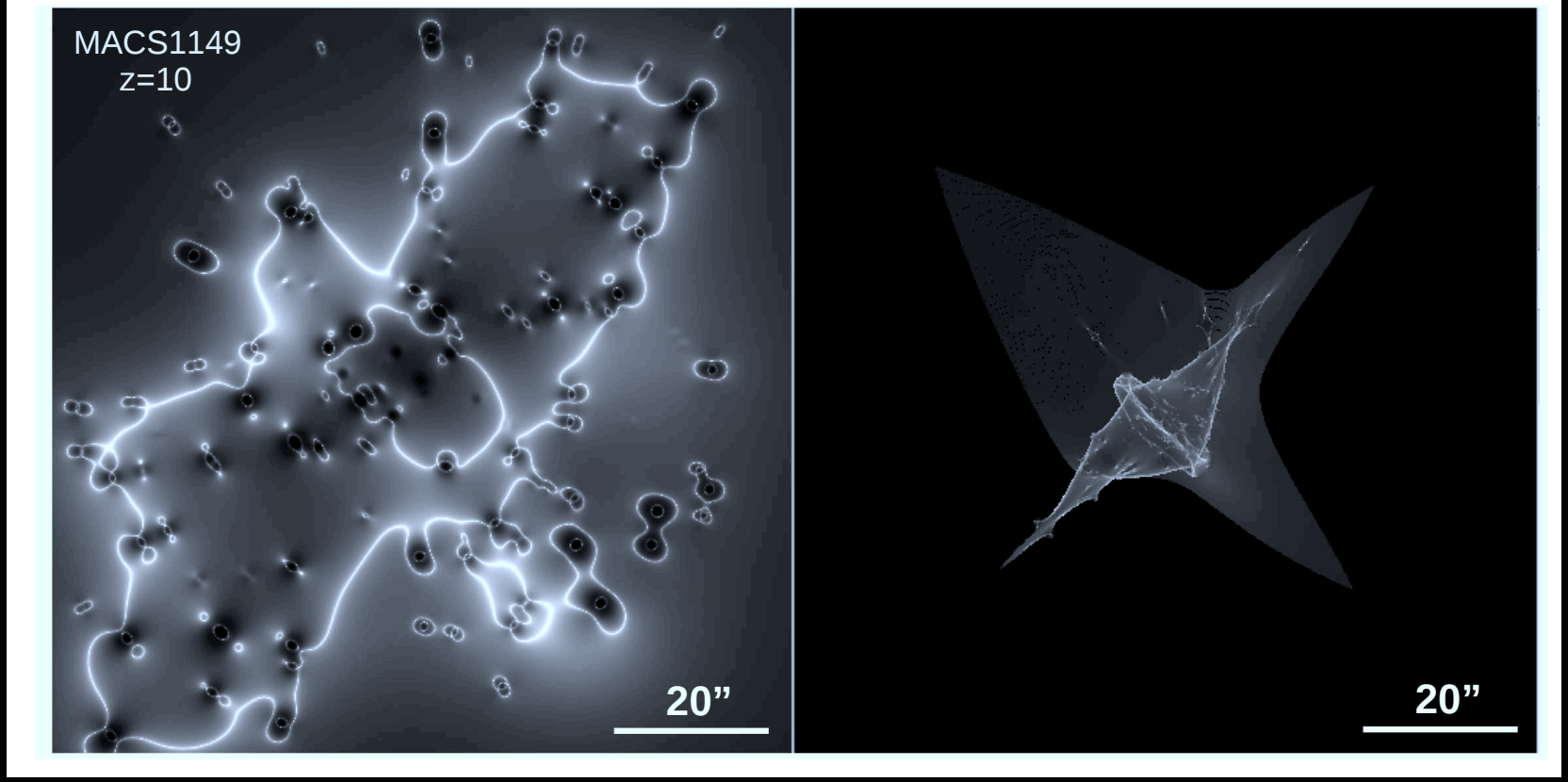

For source at z=10, critical curves for HFF cluster MACS 1149 at z≃0.54 [LEFT], and main cluster caustics [in the source plane; RIGHT].

- Transverse cluster (sub-component) velocities can be $v_T \lesssim 1000$ km/s (Kelly$^+$ 2018; Nature Astr. 2, 334; Windhorst$^+$ 2018, ApJS, 234, 41).
- Main caustic magnification $\mu \simeq 10$ $(\mathrm{d}_{caustic}/'')^{-1/2}$. For Pop III objects at z$\gtrsim$7 with 1–30 $R_\odot$, μ can then be $\gtrsim 10^4$–10^5 for $\lesssim$0.4 year.
- Must use clusters with minimal ICL near the critical curves, since ICL microlensing dilutes the main caustics (Diego$^+$ 2018, ApJ, 857, 25).

(4) HST observations of a B-star caustic transit at z≃1.49

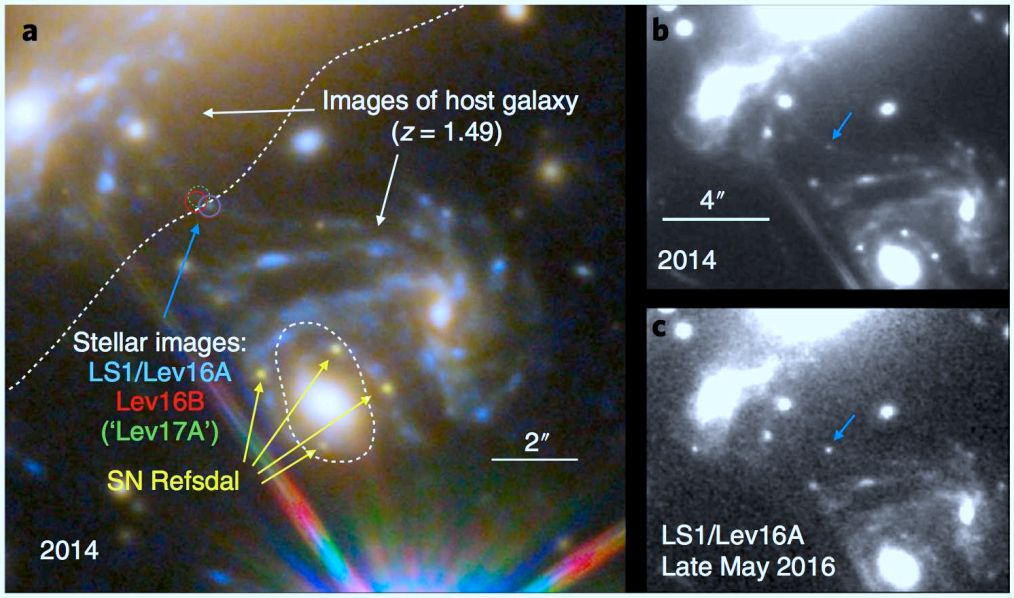

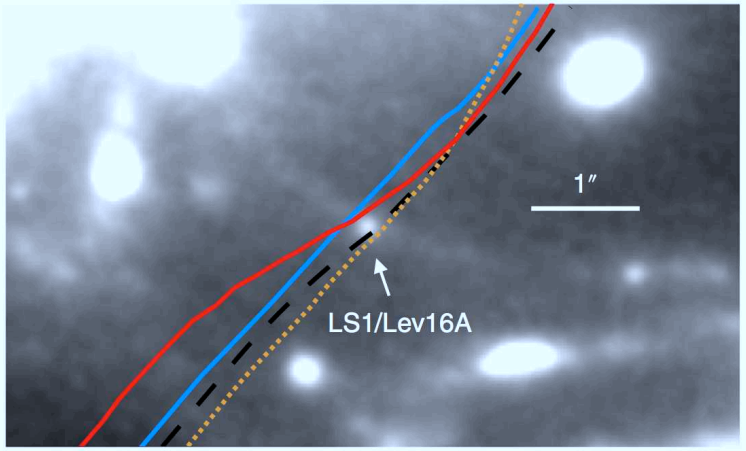

Fig. 2 | Proximity of LS1/Lev16A to the MACS J1149 galaxy cluster's critical curve for multiple galaxy-cluster lens models. Critical curves for models with available high-resolution lens maps including ref. [8] (CATS;

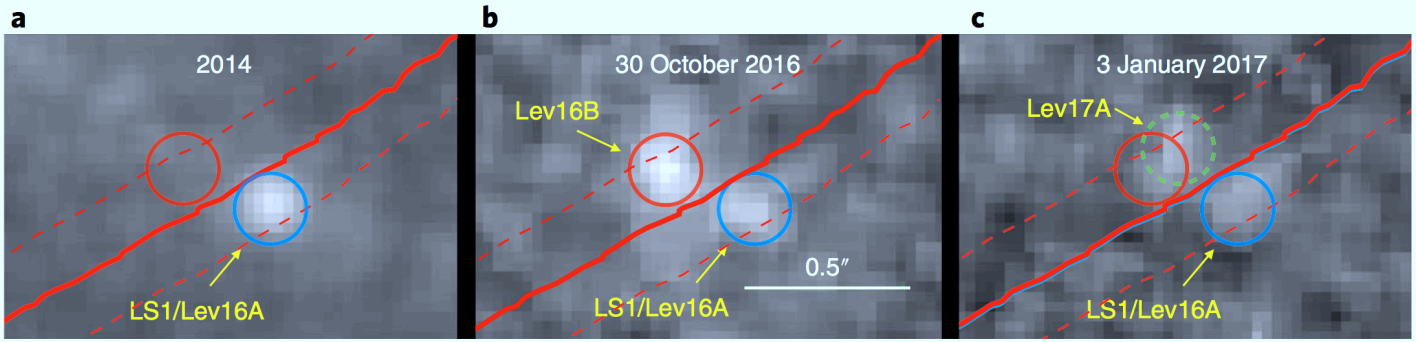

Fig. 5 | Highly magnified stellar images located near the MACS J1149 galaxy cluster's critical curve. a, LS1 in 2014; we detected LS1 when it temporarily brightened by a factor of ~4 in late April 2016, and its position is marked by a blue circle. **b**, The appearance of a new image dubbed Lev16B on 30 October 2016, whose position is marked by a red circle. The solid red line marks the location of the cluster's critical curve from the CATS cluster model[8], and the dashed red lines show the approximate 1σ uncertainty from comparison of multiple cluster lens models[5-10]. Lev16B's position is consistent with the possibility that it is a counterimage of LS1. **c**, The candidate named Lev17A at the location of the green dashed circle had a ~4σ significance detection on 3 January 2017. If a microlensing peak, Lev17A must correspond to a different star.

Kelley et al. 2018 (Nat. Astr. 2, 334): caustic transit of a B-star at z≃1.49.

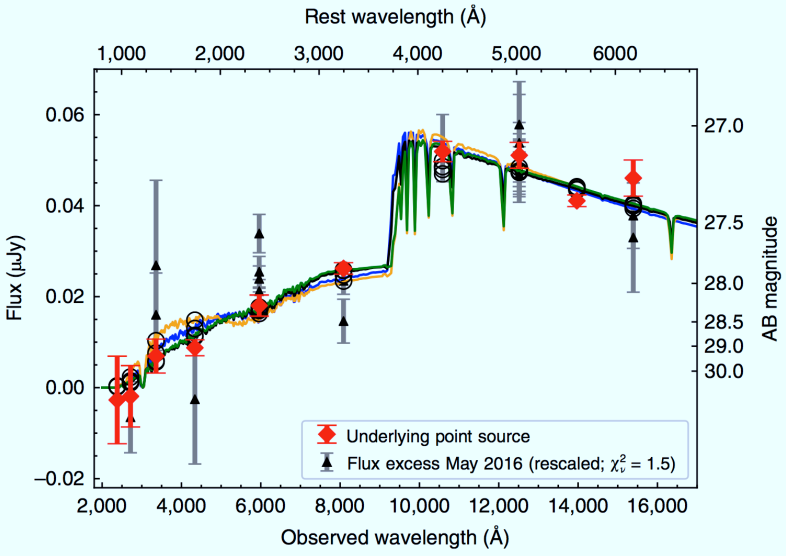

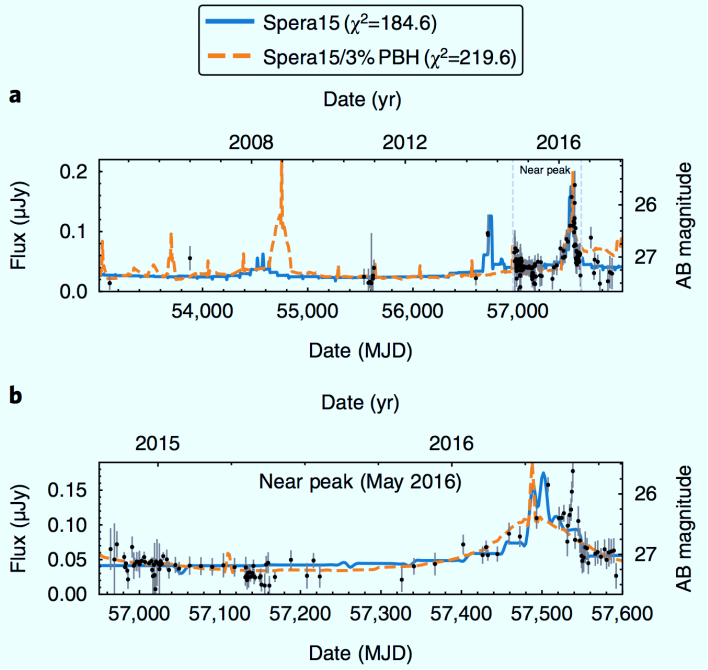

Fig. 3 | The SEDs of LS1 measured in 2013–2015 and of the rescaled excess flux density at LS1's position close to its May 2016 peak. Rescaling the SED of the flux excess (Lev16A; black triangles) to match that of the

Kelley et al. 2018 (Nat. Astr. 2, 334): caustic transit of a B-star at z≃1.49.

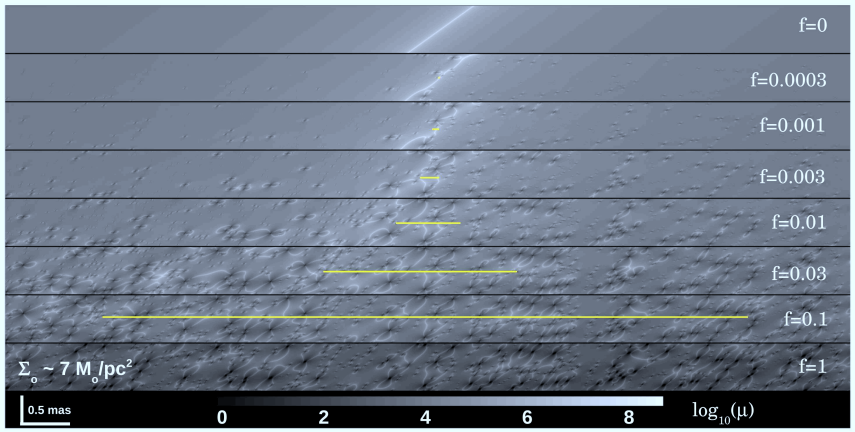

Figure 9. Disruption of the CC as a function of microlens surface mass density. Each panel shows the CC region when a population of microlenses with $\Sigma = f\Sigma_o$ is present. The case $f = 1$ corresponds to the model of Spera et al. (2015) at the position of Icarus. The yellow lines show the approximation in Equation (15). The last panel at bottom does not show the yellow line since it extends beyond the boundaries of the plot. The total surface mass density (i.e., smooth plus microlens) is the same in all panels.

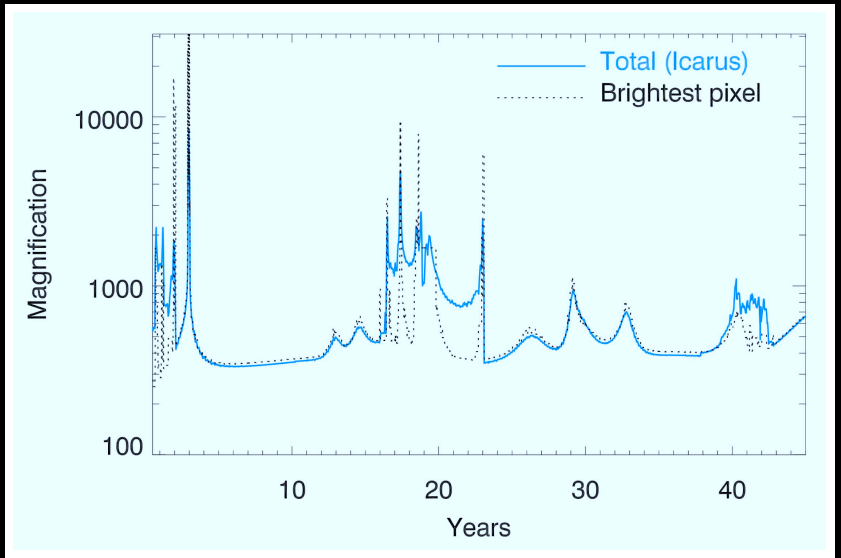

Diego+ 2018 (ApJ, 857, 25): caustic transits in the presence of microlensing.

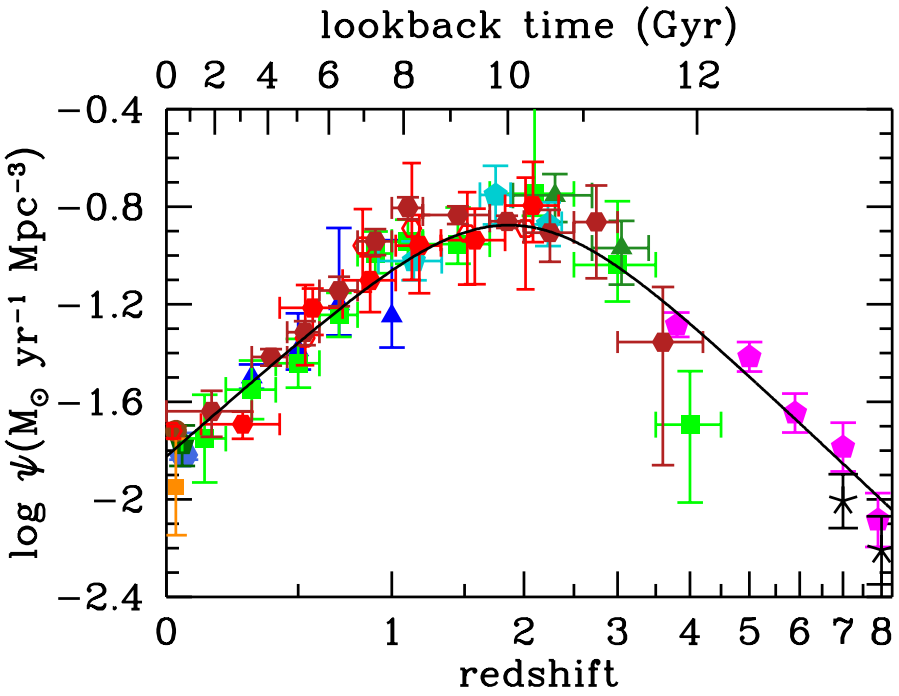

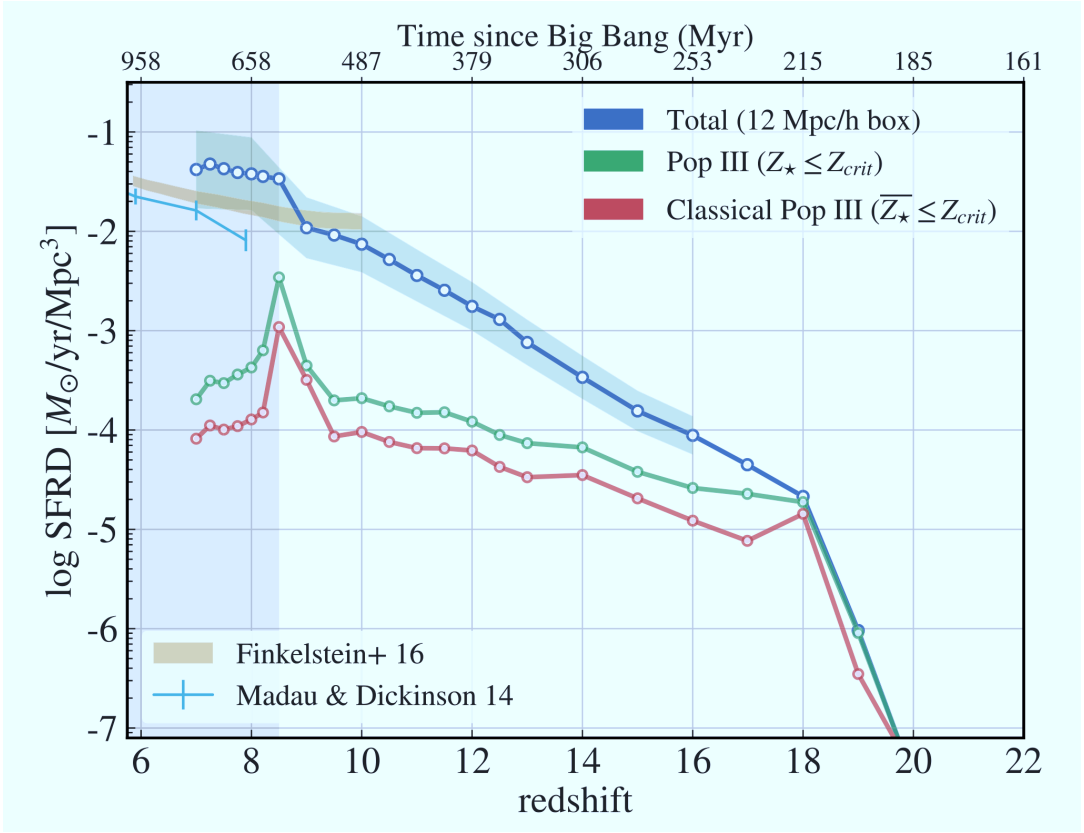

Anticipated cosmic SFR at z$\gtrsim$7:

[LEFT] Observed ($e.g.$, Madau & Dickinson; 2014 ARAA, 52, 415);
[RIGHT] RAMSES models ($e.g.$, Sarmento et al. 2018, ApJ, 854 75).

$\Rightarrow$ Adopt this SFR from z$\simeq$17 to z$\simeq$7, implying at lowest masses:

- Fe/H increases from $\sim$0 at z$\simeq$18 to 10^{-4}–10^{-3} $Z_\odot$ at z$\simeq$7.
- Integrated SFR from z$\gtrsim$7 has sky-SB(K)$\gtrsim$31 mag arcsec^{-2} (Windhorst et al. 2018), similar to the 3.6 μm CIB sky-SB possibly from BH's.

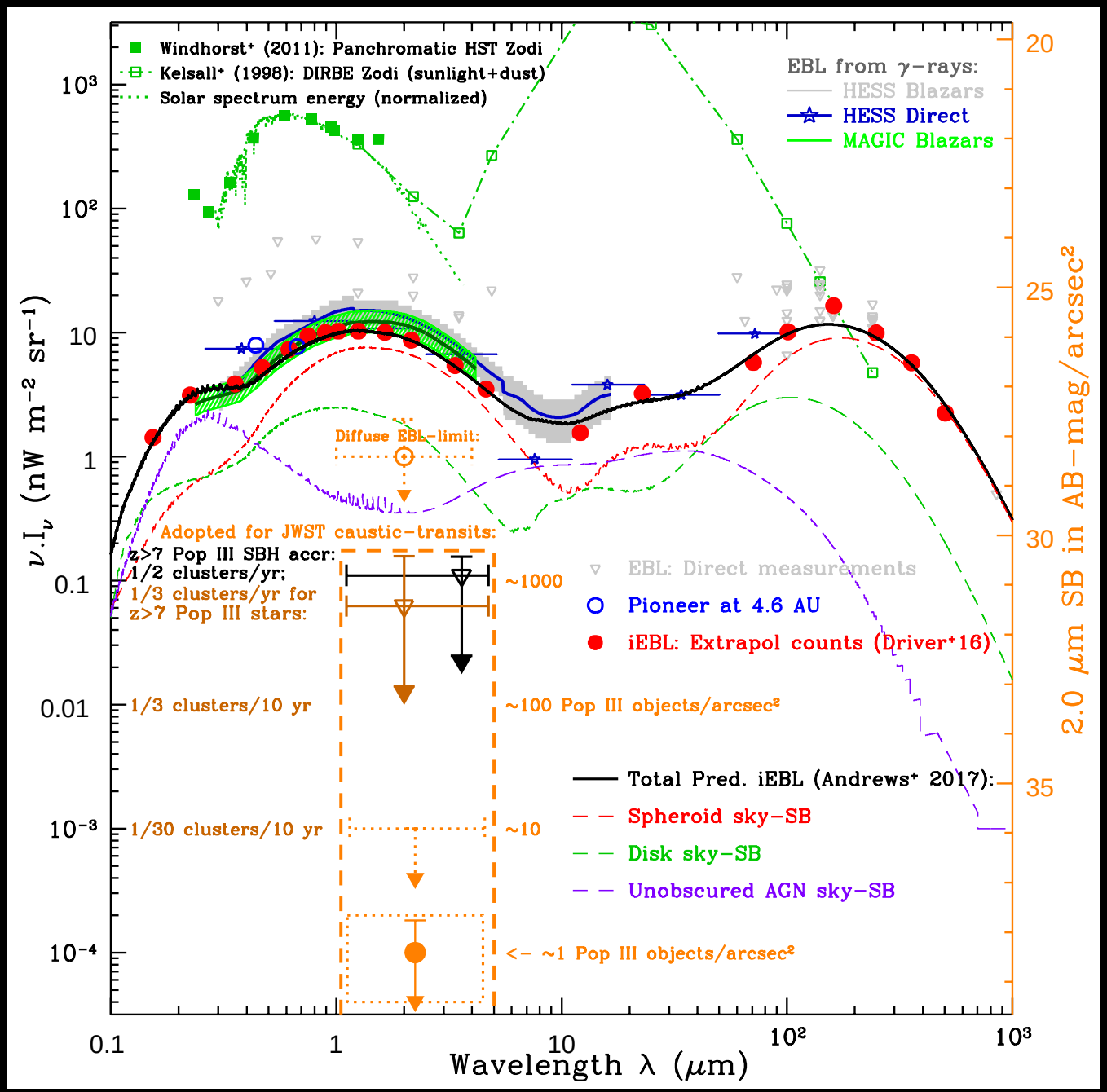

EBL constraints Driver+ 2016; Windhorst+ 2018) imply:

- Diffuse 1–4μm sky-SB $\lesssim$0.1 nW/m^2/sr (K$\gtrsim$31 mag/"^{2}), possibly from:
- 1) Pop III stars at z$\simeq$7–17, and/or
- 2) their stellar-mass BH accretion disks.

This can make Pop III stars or their BH accretion disks visible to JWST at AB$\lesssim$28–29 mag.

- Requires using the best lensing clusters and monitoring caustic transits.
- JWST must monitor best lensing clusters throughout its lifetime.

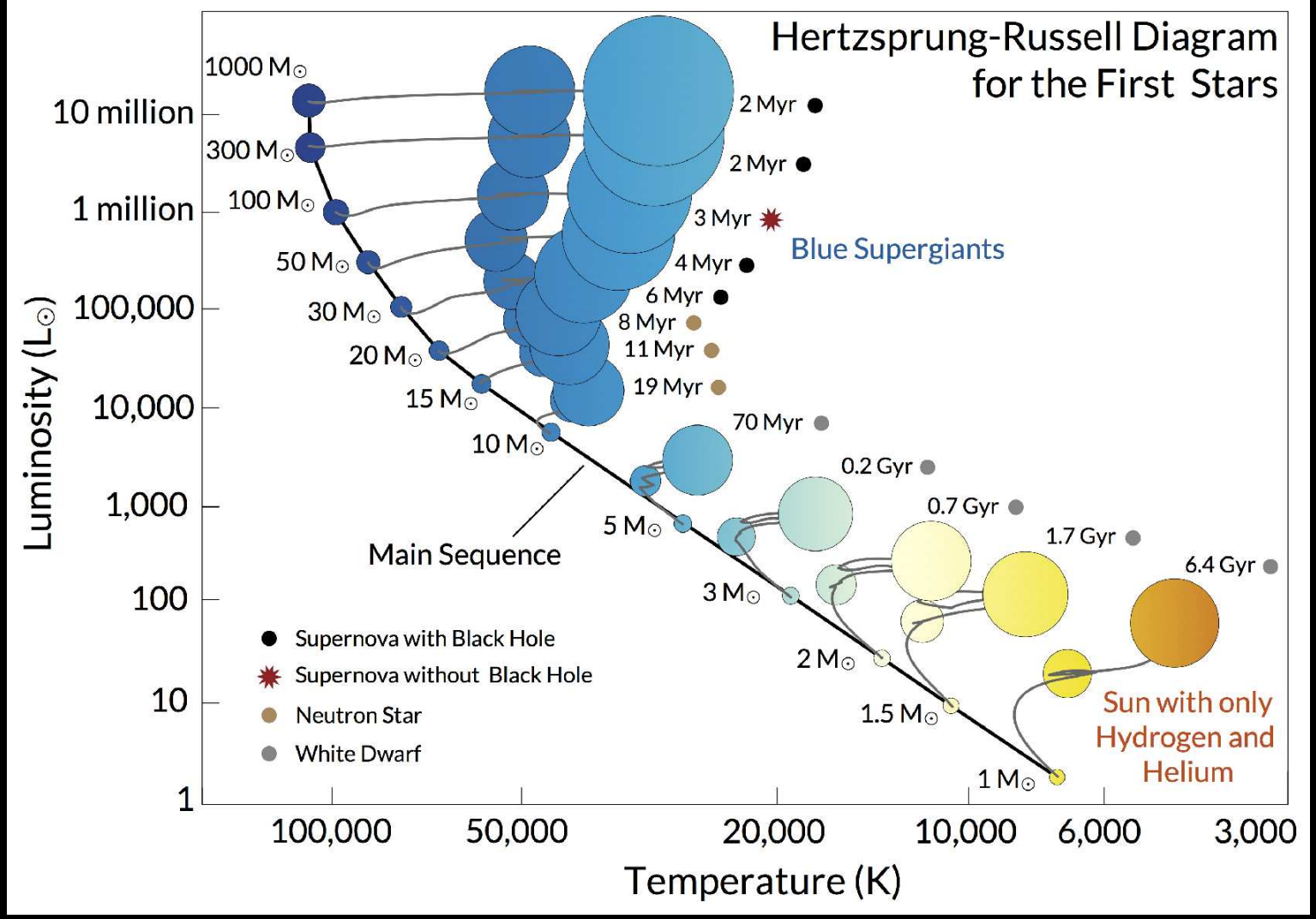

Pop III star HR-diagram: MESA stellar evolution models for z=0.0 $Z_\odot$. (Windhorst, Timmes, Wyithe et al. 2018, ApJS, 234, 41):

- 30–1000 $M_\odot$ Pop III stars (Z=0.0 $Z_\odot$) live $\sim$10$\times$ shorter than 2–5 $M_\odot$ Pop III stars in their AGB stage.
- Hence, 2–5 $M_\odot$ AGB companion stars can feed the LIGO-mass BHs left over from M$\gtrsim$30 $M_\odot$ Pop III stars (assuming binaries in 2nd generation).

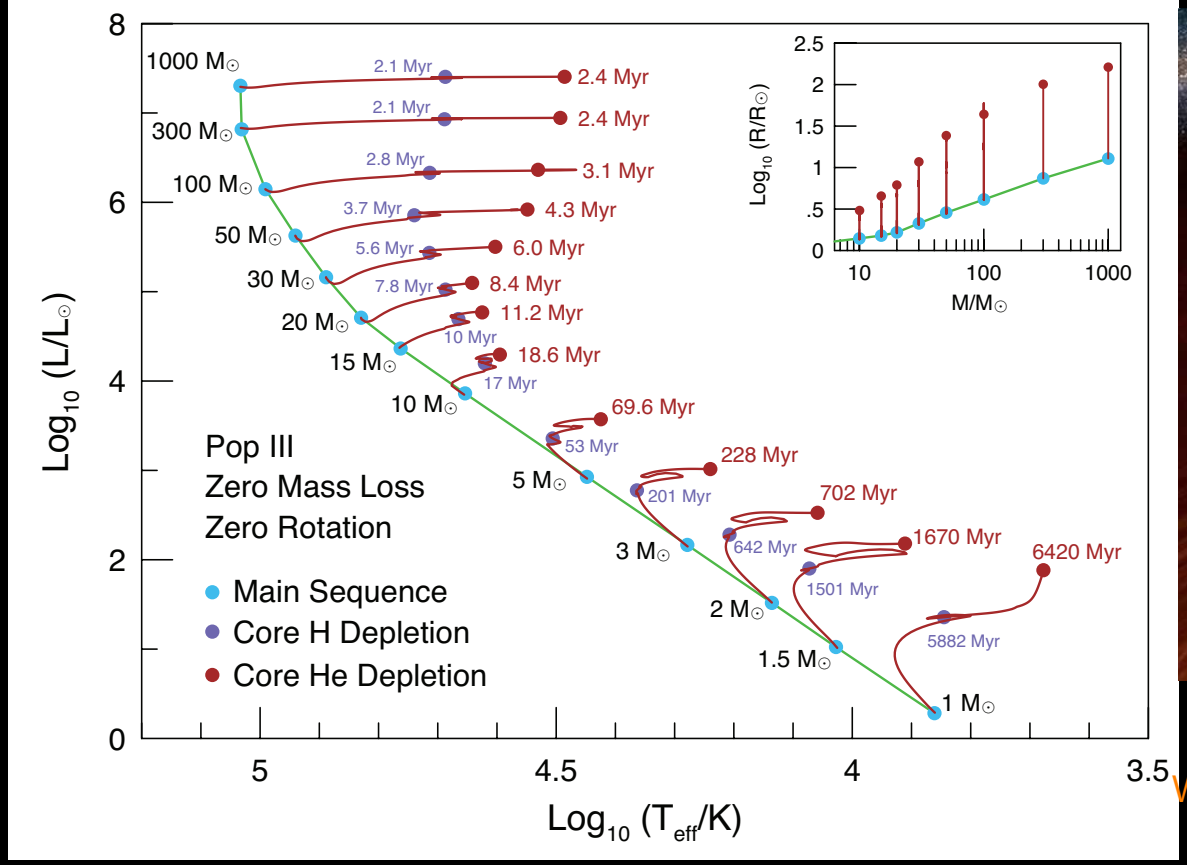

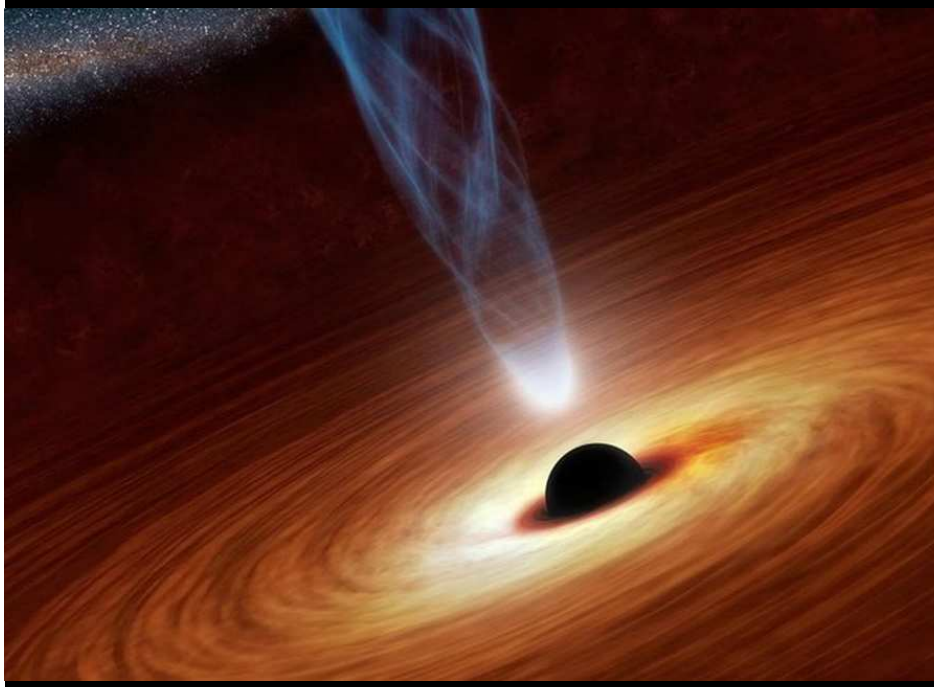

Windhorst+ (2018, ApJS, 234, 41):

- Multicolor accretion-disk models for stellar-mass black holes [RIGHT]: For $M_{BH} \simeq$5–700 $M_\odot$, accretion disks radii and luminosities are similar to those of Pop III AGB stars, when the BH is fed by a Roche lobe-filling lower-mass companion star on the AGB (which live $\gtrsim$10$\times$ longer).
- Assumes 2nd generation O-stars have high enough Fe/H ($\gtrsim 10^{-4}\ Z_\odot$) that 2–5 $M_\odot$ AGB companion stars exist and feed these LIGO-mass BHs.
- This may make stellar-mass black hole accretion disks at least as likely to be seen via caustic transits as the Pop III stars themselves.

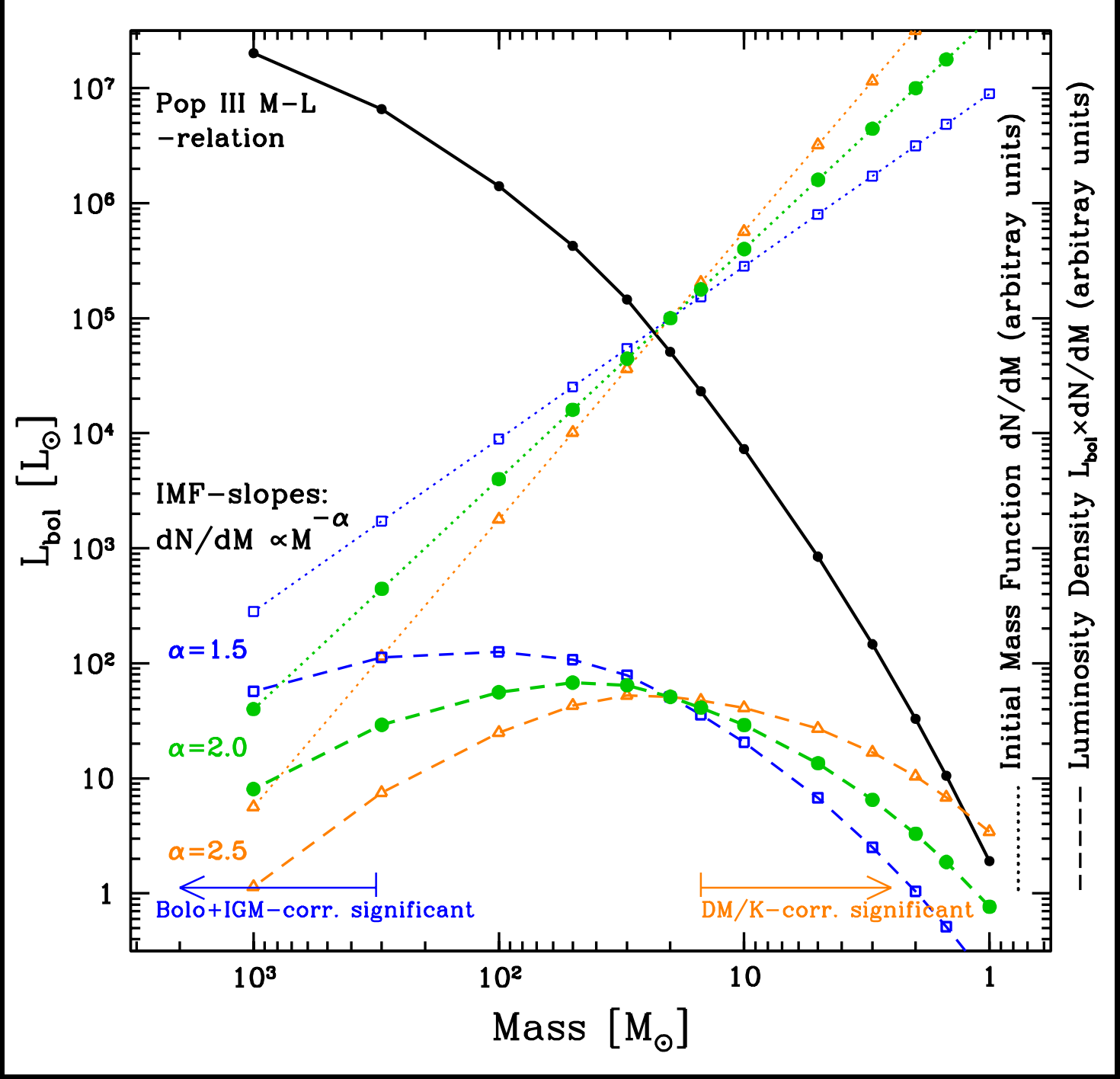

Mass–Luminosity relation for zero metallicity Pop III MESA models:

For a range of IMF slopes, most Pop III star sky-SB comes from 20–300 $M_\odot$.

Table 1. Adopted Pop III Star Physical Parameters from MESA models[a]

Mass	Age	T_{eff}	$\log R$	$\log L_{\rm bol}$	T_{eff}	$\log R$	$\log L_{\rm bol}$	Age	$T_{\rm eff}$	$\log R$	$\log L_{\rm bol}$	Age	Time[b]
	Pre-MS	— at ZAMS —			— at Hydrogen-depletion —				— at Helium-depletion —				AGB-MS
($M_\odot$)	(Myr)	(K)	($R_\odot$)	($L_\odot$)	(K)	($R_\odot$)	($L_\odot$)	Myr	(K)	($R_\odot$)	($L_\odot$)	Myr	(Myr)
1.0	9.28	7.266e3	–0.0581	0.2825	6.999e3	0.5119	1.3576	5882	—[c]	—	—	6420	538
1.5	6.11	1.065e4	–0.0203	1.0227	1.181e4	0.3292	1.9015	1501	8.149e3	0.7913	2.1804	1670	169
2.0	3.02	1.367e4	0.0108	1.5177	1.611e4	0.2498	2.2815	642	1.145e4	0.6685	2.5249	702	60
3.0	1.38	1.899e4	0.0487	2.1654	2.311e4	0.1843	2.7770	201	1.736e4	0.5510	3.0138	228	27
5.0	0.56	2.805e4	0.0911	2.9274	3.206e4	0.1903	3.3581	53	2.658e4	0.4608	3.5732	70	17
10	0.23	4.508e4	0.1462	3.8618	4.174e4	0.3807	4.1972	17	3.938e4	0.4811	4.2968	19	1.6
15	0.13	5.789e4	0.1803	4.3647	4.624e4	0.5401	4.6937	10	4.215e4	0.6581	4.7691	11	0.8
20	0.09	6.754e4	0.2183	4.7082	4.864e4	0.6612	5.0240	7.8	4.386e4	0.7879	5.0975	8.4	0.6
30	0.05	7.737e4	0.3270	5.1619	5.180e4	0.8120	5.4347	5.6	4.006e4	1.0688	5.5016	6.0	0.5
50	0.03	8.713e4	0.4570	5.6283	5.490e4	0.9722	5.8562	3.7	3.536e4	1.3862	5.9200	4.3	0.5
100	0.02	9.796e4	0.6147	6.1470	5.173e4	1.2610	6.3303	2.8	3.392e4	1.6437	6.3627	3.1	0.3
300	0.02	1.074e5	0.8697	6.8172	4.882e4	1.6111	6.9301	2.1	3.165e4	2.0041	6.9631	2.4	0.3
1000	0.02	1.080e5	1.1090	7.3047	4.807e4	1.8740	7.4288	2.1	3.122e4	2.2119	7.3549	2.4	0.3

Windhorst, Timmes, Wyithe et al. (2018, ApJS, 234, 41):

- 30–1000 $M_\odot$ Pop III stars (Z=0.0 $Z_\odot$) live ∼10× shorter than 2–5 $M_\odot$ Pop III stars in their AGB stage.
- Hence, 2–5 $M_\odot$ AGB companion stars can feed the LIGO-mass BHs left over from M≳30 $M_\odot$ Pop III stars (assuming binaries in 2nd generation).

Table 2. Implied ZAMS Pop III Star Observational Parameters Relevant to Caustic Transit Calculations

Mass[a]	$T_{\rm eff}$[b]	Radius[c]	$L_{\rm bol}$[d]	$M_{\rm bol}$[e]	Bolo+IGM+K-corr[f]			ZAMS $m_{\rm UV}$[g]			t_{rise}[h]	transit[i]
ZAMS		— at ZAMS —			z=7	z=12	z=17	z=7	z=12	z=17	caust	rate
($M_\odot$)	(K)	($R_\odot$)	($L_\odot$)	(AB)	(AB-mag)			(AB-mag)			(hr)	(/cl/yr)
1.0	7.266e3	0.87	1.92	+4.03	+4.44	+3.13	+2.61	57.71	57.74	58.07	0.17	8×10^5
1.5	1.065e4	0.95	10.5	+2.18	+1.45	+0.42	–0.06	52.87	53.18	53.55	0.18	1.1×10^4
2.0	1.367e4	1.03	32.9	+0.95	+0.30	–0.59	–1.06	50.49	50.93	51.31	0.20	1.5×10^3
3.0	1.899e4	1.12	146.	–0.67	–0.51	–1.26	–1.72	48.06	48.64	49.03	0.22	182.
5.0	2.805e4	1.23	846.	–2.58	–0.70	–1.35	–1.80	45.96	46.65	47.04	0.24	29.1
10	4.508e4	1.40	7.28e3	–4.91	–0.22	–0.79	–1.23	44.10	44.88	45.27	0.27	5.70
15	5.789e4	1.51	2.32e4	–6.17	+0.23	–0.30	–0.75	43.30	44.10	44.50	0.29	2.78
20	6.754e4	1.65	5.11e4	–7.03	+0.56	+0.04	–0.40	42.77	43.59	43.99	0.32	1.74
30	7.737e4	2.12	1.45e5	–8.16	+0.88	+0.36	–0.08	41.95	42.78	43.17	0.41?	0.82?
50	8.713e4	2.86	4.25e5	–9.33	+1.17	+0.66	+0.22	41.08	41.91	42.31	0.55*	0.37*
100	9.796e4	4.12	1.40e6	–10.63	+1.47	+0.96	+0.52	40.08	40.91	41.31	0.80*	0.15*
300	1.074e5	7.41	6.56e6	–12.30	+1.71	+1.21	+0.77	38.64	39.48	39.88	1.43*	0.039*
1000	1.080e5	12.9	2.02e7	–13.52	+1.72	+1.22	+0.78	37.44	38.28	38.68	2.48*	0.013*

- If M$\gtrsim$30 $M_\odot$ Pop III ZAMS stars have $\mu\gtrsim10^4$–10^5 during caustic transits, they could be detectable for months to AB$\lesssim$29 mag with JWST.
- Expect $\lesssim$1 caustic transit/yr at z$\gtrsim$7 when JWST monitors $\gtrsim$3 clusters.

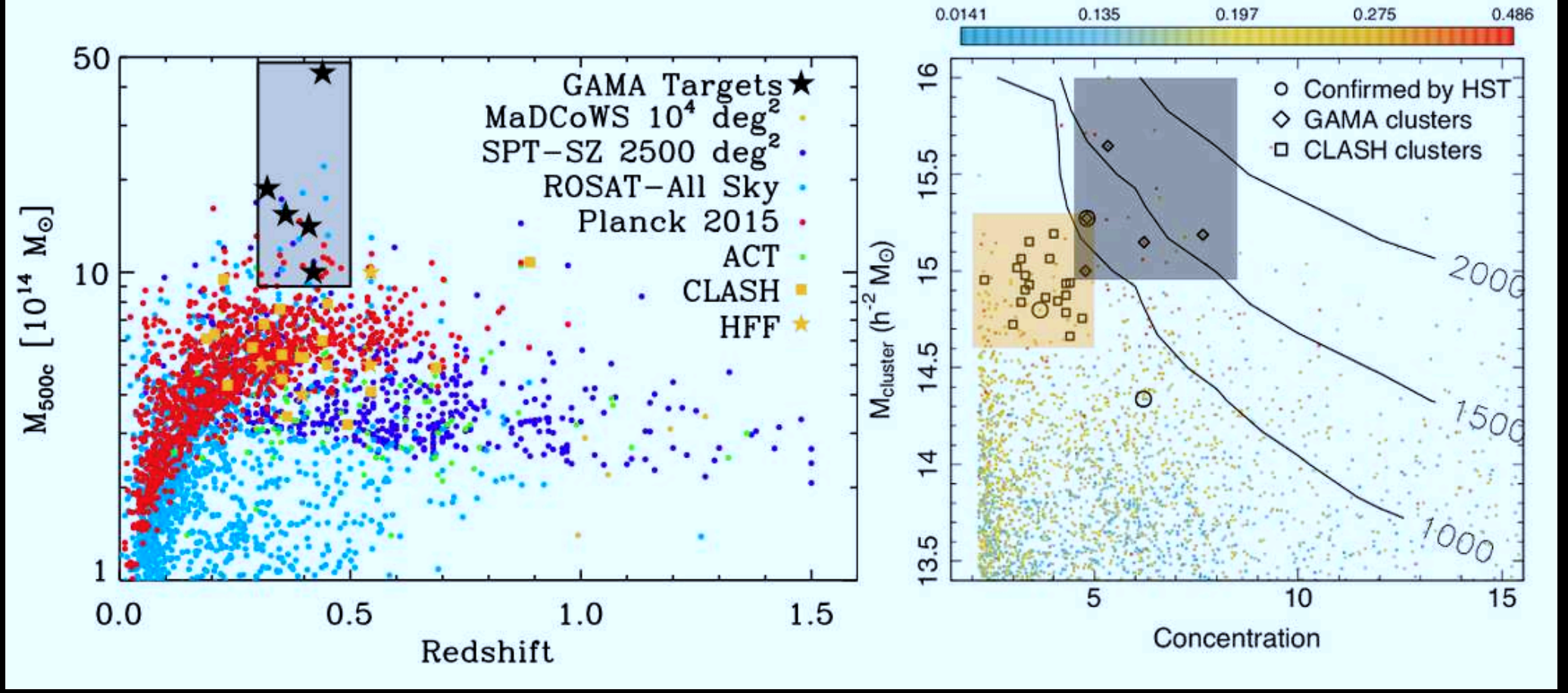

What are the best lensing clusters for JWST to see First Light objects?:

[LEFT] Best lensing clusters vs. ROSAT, Planck, SPT, MaDCoWS.

[RIGHT] Best lensing clusters compared to CLASH clusters.

(Contours: Number of lensed JWST sources at $z \simeq 1$–15 to AB$\lesssim$31 mag).

- Resulting sweet spot for JWST lensing of First Light Objects ($z \gtrsim 10$):

Redshift: $0.3 \lesssim z \lesssim 0.5$; Mass: $10^{15-15.6}\ M_\odot$; Concentration: $4.5 \lesssim C \lesssim 8.5$

(4) What are the best lensing clusters to monitor caustic transits?

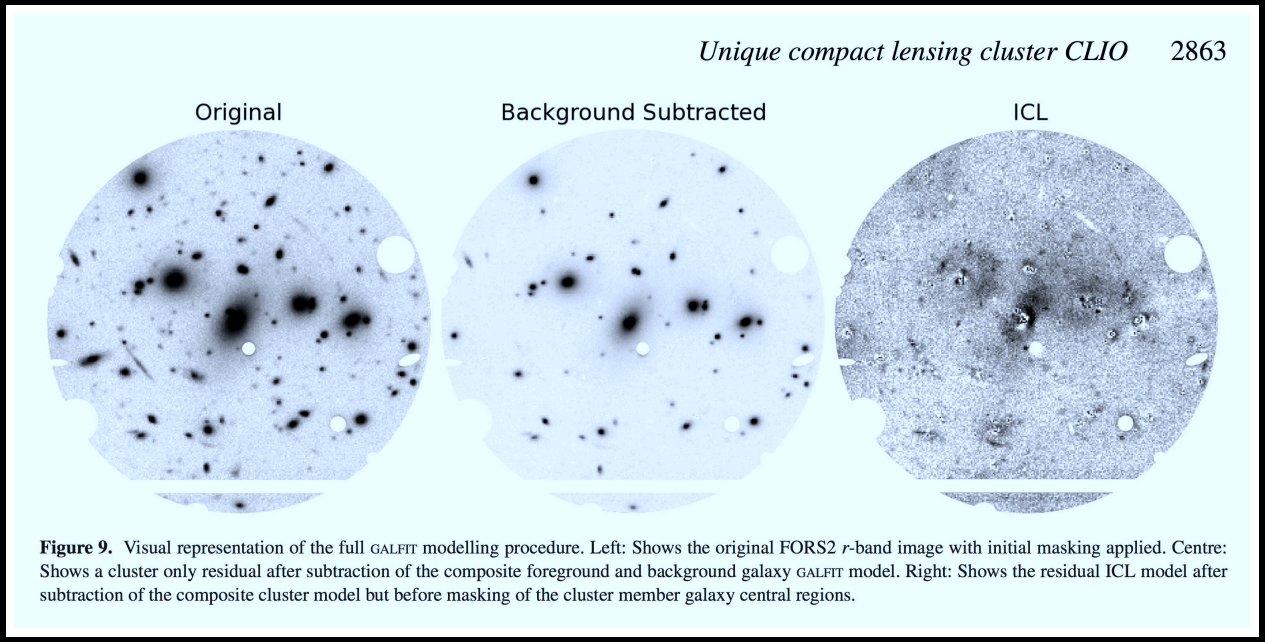

Figure 9. Visual representation of the full GALFIT modelling procedure. Left: Shows the original FORS2 *r*-band image with initial masking applied. Centre: Shows a cluster only residual after subtraction of the composite foreground and background galaxy GALFIT model. Right: Shows the residual ICL model after subtraction of the composite cluster model but before masking of the cluster member galaxy central regions.

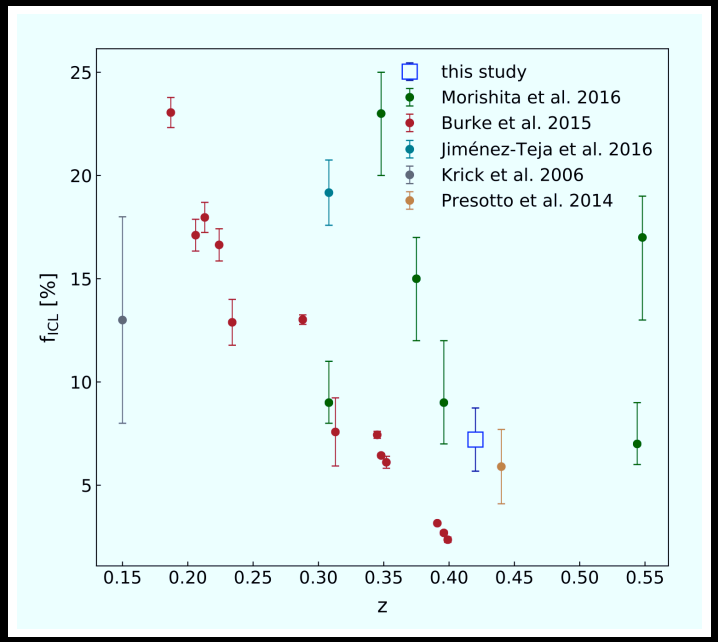

Griffiths et al. (2018 MNRAS, 475, 2853): GAMA cluster at z≃0.42 found through mass-concentration selection. Has 89 VLT MUSE members:

- Cluster has minimal ICL near the critical curves, optimal for caustic transit studies. Can see several arcs clearly in ground-based images.
- JWST should monitor clusters with minimal ICL near the critical curves to minimize microlensing and maximize caustic transit magnifications.

Conclusions for Pop III stars/BH accretion disks caustic transits

- If M$\gtrsim$30 $M_\odot$ Pop III ZAMS stars (AB$\sim$37–42 mag at z$\gtrsim$7) have $\mu\gtrsim10^4$–10^5 during caustic transits, they could be detectable for a few months to AB$\lesssim$29 mag with JWST. Rise times of a few hours.

- Pop III RGB and AGB stars have more advantageous combined Bolometric +IGM+K-corrections, and could be 1–2 mag brighter, but live $\sim$10$\times$ shorter than ZAMS stars.

- Pop III stellar mass black hole (M$\gtrsim$20 $M_\odot$) accretion disks also could be $\sim$1 mag brighter *and* live $\sim$10$\times$ longer than their ZAMS stars.

- JWST could detect *both* Pop III stars and their stellar-mass BH (M$\gtrsim$20 $M_\odot$) accretion disks at AB$\lesssim$28-29 mag via cluster caustic transits if magnification $\mu\simeq10^4$–10^5 (*i.e.*, ICL microlensing doesn't dominate caustics).

- Expect $\lesssim$1 caustic transit/yr at z$\gtrsim$7 when JWST monitors $\gtrsim$3 clusters.

- Stellar-mass BH accretion disks may dominate caustic transits at z$\gtrsim$7.

- JWST GO community should anticipate this, and plan for it.

SPARE CHARTS

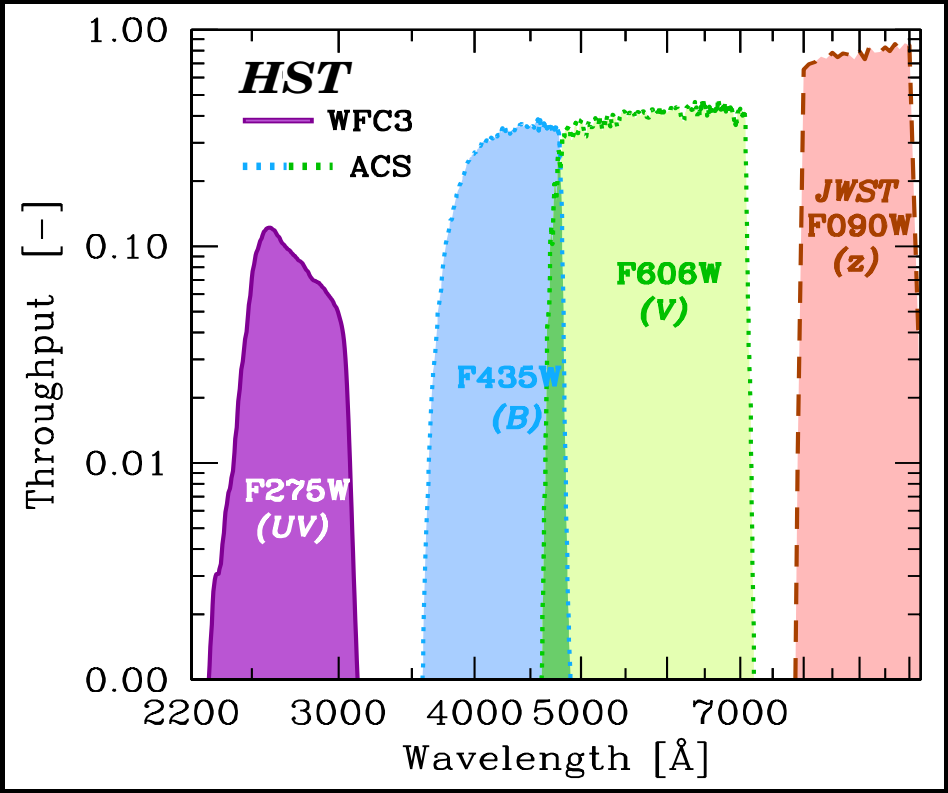

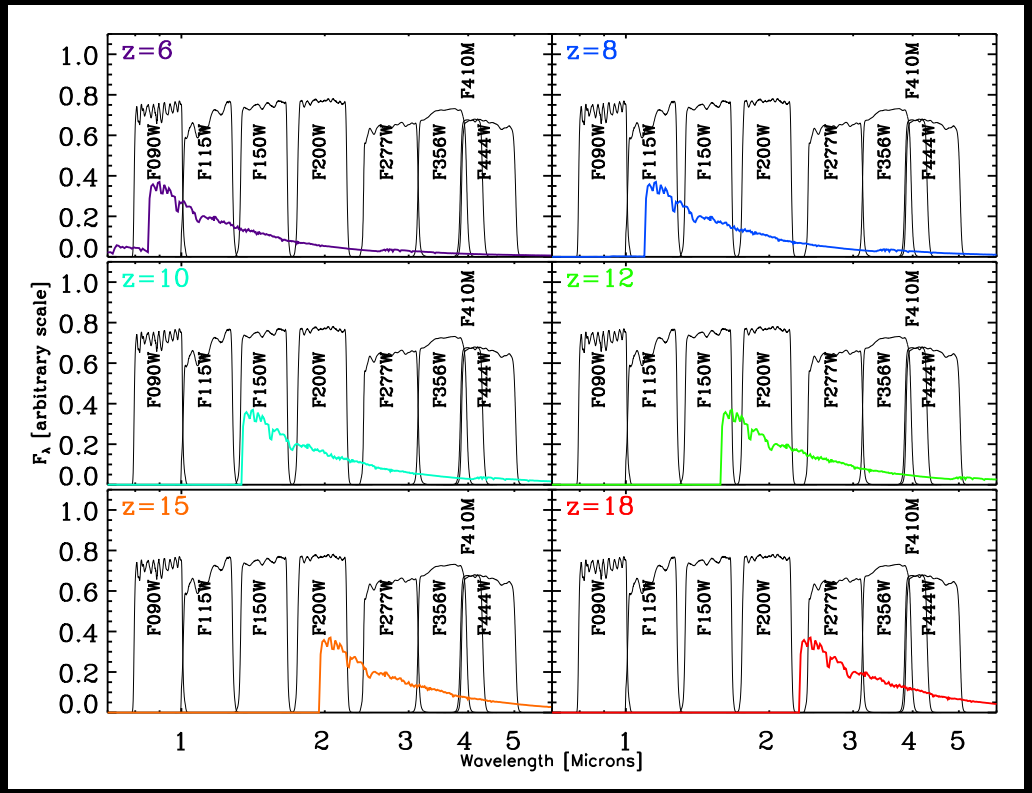

[LEFT] HST UV-vis filters complement the JWST NEP community field:

- HST adds λ's inaccessible to JWST, or where HST has better PSF.

[RIGHT] Standard 8-band 0.8–5 μm filter set for JWST NIRCam.

- These are what GTO's will use as standard NIRCam filters.

Table 3. Implied Red Giant Branch Pop III Star Observational Parameters Relevant to Caustic Transit Calculations

Mass[a]	$T_{\rm eff}$[b]	Radius[c]	$L_{\rm bol}$[d]	$M_{\rm bol}$[e]	Bolo+IGM+K-corr[f]			Giant Branch $m_{\rm UV}$[g]			t_{rise}[h]	transit[i]
GB	— at Hydrogen-depletion —				z=7	z=12	z=17	z=7	z=12	z=17	caust	rate
($M_\odot$)	(K)	($R_\odot$)	($L_\odot$)	(AB)	(AB-mag)			(AB-mag)			(hr)	(/cl/yr)
1.0	6.999e3	3.25	22.8	+1.35	+4.83	+3.48	+2.96	55.42	55.41	55.73	0.63	9×10^4
1.5	1.181e4	2.13	79.7	–0.01	+0.91	–0.06	–0.53	50.13	50.51	50.88	0.41	1.0×10^3
2.0	1.611e4	1.78	191.	–0.96	–0.19	–1.01	–1.47	48.08	48.60	48.99	0.34	175.
3.0	2.311e4	1.53	598.	–2.20	–0.69	–1.39	–1.84	46.35	46.99	47.38	0.30	39.8
5.0	3.206e4	1.55	2.28e3	–3.66	–0.63	–1.25	–1.70	44.95	45.67	46.07	0.30	11.8
10	4.174e4	2.40	1.57e4	–5.75	–0.34	–0.92	–1.36	43.15	43.91	44.31	0.46	2.33
15	4.624e4	3.47	4.94e4	–6.99	–0.18	–0.74	–1.19	42.06	42.84	43.24	0.67?	0.87?
20	4.864e4	4.58	1.06e5	–7.82	–0.10	–0.65	–1.09	41.32	42.11	42.51	0.88*	0.44*
30	5.180e4	6.49	2.72e5	–8.85	+0.02	–0.53	–0.97	40.41	41.20	41.60	1.25*	0.19*
50	5.490e4	9.38	7.18e5	–9.90	+0.13	–0.42	–0.86	39.47	40.26	40.66	1.81*	0.081*
100	5.173e4	18.2	2.14e6	–11.09	+0.02	–0.53	–0.98	38.17	38.96	39.36	3.52*	0.024*
300	4.882e4	40.8	8.51e6	–12.59	–0.09	–0.65	–1.09	36.57	37.35	37.75	7.88*	0.006*
1000	4.807e4	74.8	2.68e7	–13.83	–0.12	–0.67	–1.12	35.29	36.07	36.47	14.44*	0.002*

- If M$\gtrsim$20 $M_\odot$ Pop III RGB stars have $\mu\gtrsim10^4$–10^5 during caustic transits, they could be detectable for a few months to AB$\lesssim$29 mag with JWST.
- Note the combined Bolometric+IGM+K-corrections are more advantageous for Pop III RGB stars.

Table 4. Implied AGB Pop III Star Observational Parameters Relevant to Caustic Transit Calculations

Mass[a]	$T_{\rm eff}$[b]	Radius[c]	$L_{\rm bol}$[d]	$M_{\rm bol}$[e]	Bolo+IGM+K-corr[f]			AGB $m_{\rm UV}$[g]			t_{rise}[h]	transit[i]
AGB	— at Helium-depletion —				z=7	z=12	z=17	z=7	z=12	z=17	caust	rate
($M_\odot$)	(K)	($R_\odot$)	($L_\odot$)	(AB)	(AB-mag)			(AB-mag)			(hr)	(/cl/yr)
1.0	6.312e3[j]	5.23[j]	39.8[j]	+0.74	+6.01	+4.57	+4.03	55.99	55.89	56.19	1.01	1.4×10^5
1.5	8.149e3	6.18	151.	–0.71	+3.36	+2.14	+1.64	51.89	52.01	52.35	1.19	4.0×10^3
2.0	1.145e4	4.66	335.	–1.57	+1.06	+0.07	–0.40	48.73	49.08	49.45	0.90	273.
3.0	1.736e4	3.56	1.03e3	–2.79	–0.36	–1.15	–1.60	46.09	46.64	47.03	0.69	28.9
5.0	2.658e4	2.89	3.74e3	–4.19	–0.72	–1.38	–1.82	44.33	45.01	45.41	0.56	6.43
10	3.938e4	3.03	1.98e4	–6.00	–0.42	–1.00	–1.45	42.82	43.57	43.97	0.58	1.71
15	4.215e4	4.55	5.88e4	–7.18	–0.33	–0.90	–1.34	41.73	42.50	42.89	0.88?	0.64?
20	4.386e4	6.14	1.25e5	–8.00	–0.27	–0.84	–1.28	40.97	41.74	42.14	1.19*	0.32*
30	4.006e4	11.7	3.17e5	–9.01	–0.40	–0.98	–1.42	39.83	40.59	40.98	2.26*	0.11*
50	3.536e4	24.3	8.32e5	–10.06	–0.55	–1.15	–1.59	38.63	39.37	39.77	4.70*	0.036*
100	3.392e4	44.0	2.31e6	–11.17	–0.59	–1.19	–1.64	37.49	38.22	38.61	8.50*	0.012*
300	3.165e4	101.	9.19e6	–12.67	–0.64	–1.26	–1.71	35.93	36.65	37.04	19.49*	0.003*
1000	3.122e4	163.	2.26e7	–13.65	–0.65	–1.28	–1.72	34.94	35.66	36.05	31.45*	0.001*

- If M$\gtrsim$20 $M_\odot$ Pop III AGB stars have $\mu\gtrsim10^4$–10^5 during caustic transits, they could be detectable for a few months to AB$\lesssim$29 mag with JWST.
- Note the combined Bolometric+IGM+K-corrections are far more advantageous for Pop III AGB stars (especially at z$\gtrsim$12)!

Table 5. Pop III Stellar Mass Black Hole Accretion Disk Parameters Adopted for Caustic Transit Calculations

Mass[a] ZAMS ($M_\odot$)	$M_{compact}$[b] ($M_\odot$)	R_s[c] BH (km)	Radius[d] ($R_\odot$)	L_{bol}[e] ($L_\odot$)	M_{bol}[f] AB-mag	bolo+IGM+K-corr[g] z=7	z=12	z=17	m_{AB}-limits at[h] z=7	z=12	z=17	t_{rise}[i] (z=12) (hr)	Transit[j] rate (/cl/yr)
— of the UV accretion disk —						(AB-mag)			(AB-mag)				
BH accretion-disk bolometric luminosities and UV half-light radii scaling from microlensed quasars (Blackburne et al. 2011)													
30	~5.0 BH	15	1.4	$\lesssim 4.2\times10^4$	$\gtrsim$–6.8	–0.6	–1.4	–1.7	$\gtrsim$41.8	$\gtrsim$42.4	$\gtrsim$42.9	0.27?	$\gtrsim$0.58?
50	~24 BH	72	3.0	$\lesssim 2.0\times10^5$	$\gtrsim$–8.5	–0.4	–1.2	–1.5	$\gtrsim$40.3	$\gtrsim$40.9	$\gtrsim$41.4	0.58*	$\gtrsim$0.15*
100	~65 BH	195	4.9	$\lesssim 5.4\times10^5$	$\gtrsim$–9.6	–0.2	–0.9	–1.3	$\gtrsim$39.4	$\gtrsim$40.0	$\gtrsim$40.5	0.95*	$\gtrsim$0.06*
300	~230 BH	690	9.2	$\lesssim 1.9\times10^6$	$\gtrsim$–11.0	–0.2	–1.0	–1.3	$\gtrsim$38.1	$\gtrsim$38.6	$\gtrsim$39.2	1.8*	$\gtrsim$0.02*
1000	~720 BH	2160	16.3	$\lesssim 6.0\times10^6$	$\gtrsim$–12.2	–0.2	–0.9	–1.3	$\gtrsim$36.8	$\gtrsim$37.5	$\gtrsim$37.9	3.2*	$\gtrsim$0.01*
BH accretion-disk bolometric luminosities and UV half-light radii estimated from multi-color thin-disk model													
30	~5.0 BH	15	1.9	$\lesssim 3.1\times10^4$	$\gtrsim$–6.5	–0.6	–1.4	–1.7	$\gtrsim$42.1	$\gtrsim$42.8	$\gtrsim$43.2	0.37?	$\gtrsim$0.84?
50	~24 BH	72	4.5	$\lesssim 1.8\times10^5$	$\gtrsim$–8.4	–0.4	–1.2	–1.5	$\gtrsim$40.4	$\gtrsim$41.1	$\gtrsim$41.5	0.87*	$\gtrsim$0.18*
100	~65 BH	195	7.8	$\lesssim 5.9\times10^5$	$\gtrsim$–9.7	–0.2	–0.9	–1.3	$\gtrsim$39.3	$\gtrsim$40.0	$\gtrsim$40.4	1.51*	$\gtrsim$0.06*
300	~230 BH	690	15.8	$\lesssim 2.0\times10^6$	$\gtrsim$–11.0	–0.2	–1.0	–1.3	$\gtrsim$38.0	$\gtrsim$38.6	$\gtrsim$39.1	3.1*	$\gtrsim$0.02*
1000	~720 BH	2160	29.8	$\lesssim 6.6\times10^6$	$\gtrsim$–12.3	–0.2	–0.9	–1.3	$\gtrsim$36.7	$\gtrsim$37.4	$\gtrsim$37.8	5.8*	$\gtrsim$0.01*

- If M$\gtrsim$20 $M_\odot$ Pop III stellar mass black hole accretion disks have $\mu\gtrsim10^4$–10^5 during caustic transits, they could be detectable for a few months to AB$\lesssim$29 mag with JWST. Rise times ~hours–1 day; Decay times $\lesssim$0.4 yr.
- Note the combined Bolometric+IGM+K-corrections are also more advantageous for Pop III stellar-mass black hole accretion disks.

Multi-λ model: $T\propto r^{-3/4}$; $T_{max}\simeq10\left(\frac{M_{BH}}{100}\right)^{-3/8}$ *keV*; $r_{hl}\propto M_{BH}{}^{1/2}$.

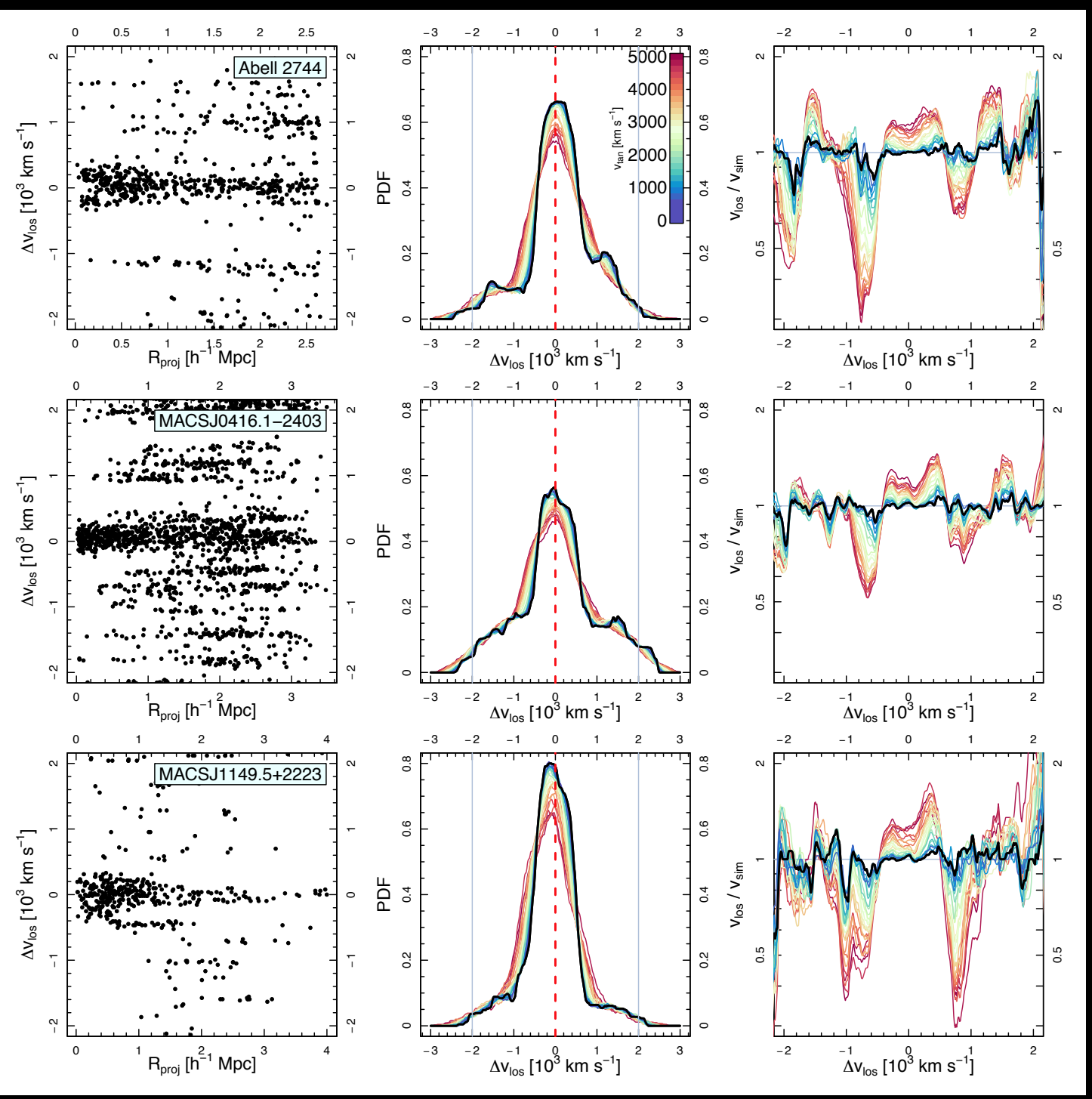

Trumpet diagrams for JWST lensing clusters from ground-based spectroscopic N(z) (Windhorst$^+$ 2018):

- 1) Add random *space* velocity v_{sp} to clusters.
- 2) Projected v_T must be $\lesssim$1000km/s for v_{sp} not to unduly disturb radial N(z).
- 3) Best clusters (Bullet) for caustic transits can have $v_T \lesssim 2700$ km s^{-1}.

- JWST should monitor such clusters during its lifetime for caustic transits.

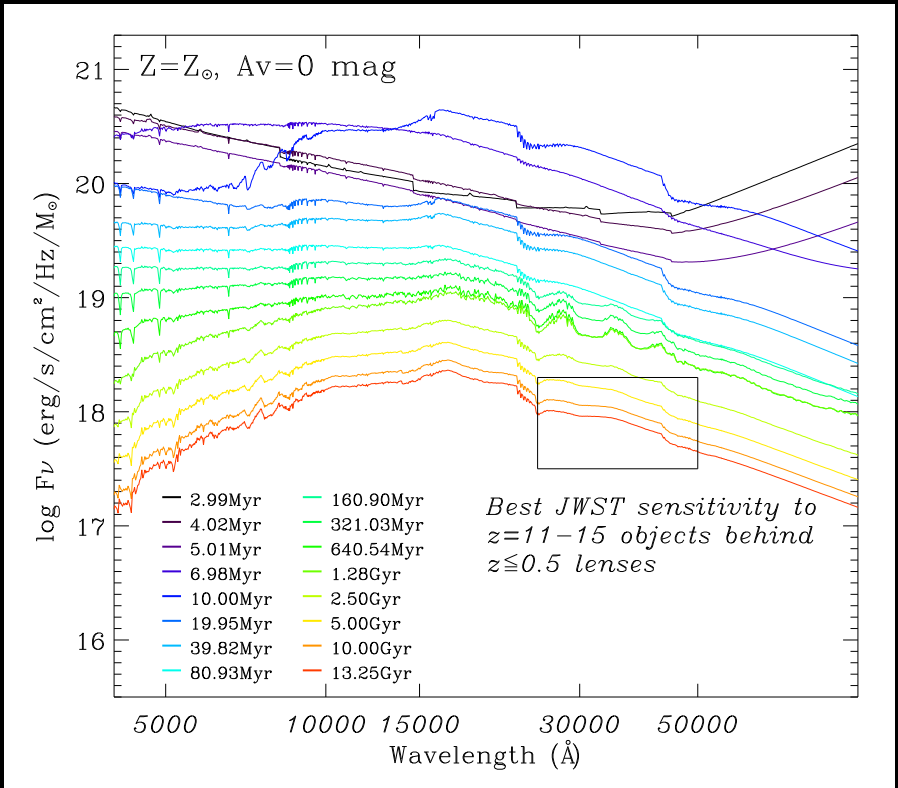

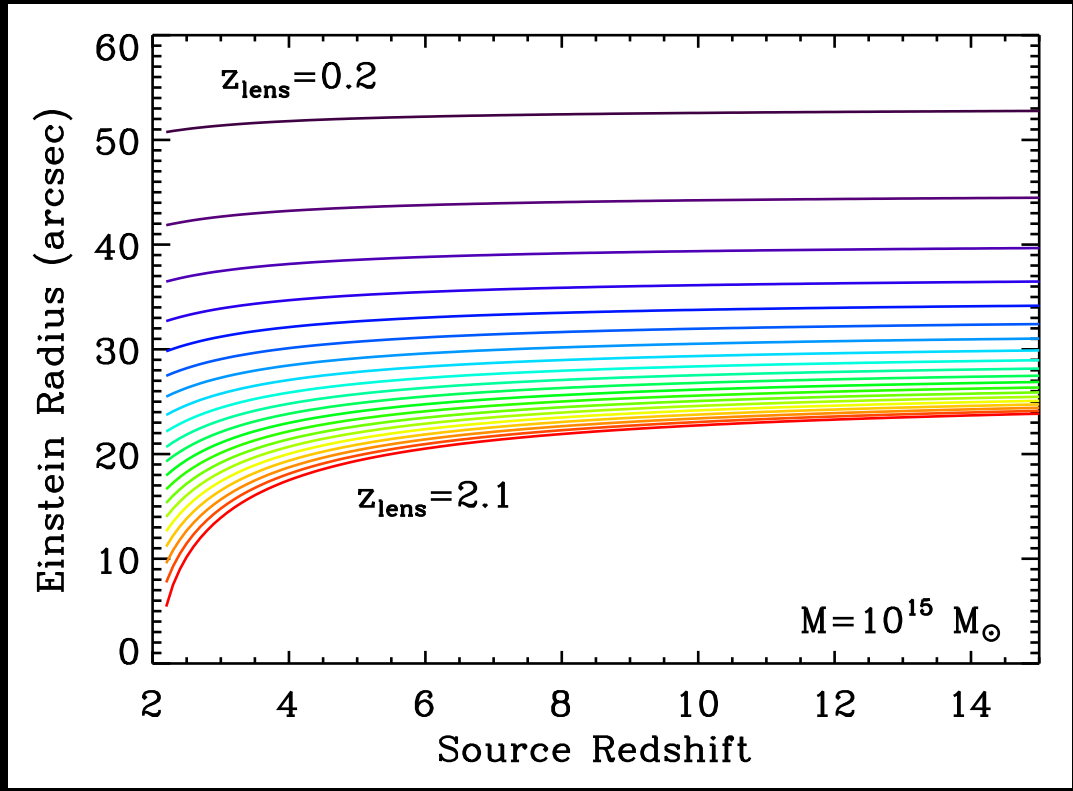

Galaxy SEDs for different ages: peak at $\lambda_{rest} \simeq 1.6\mu$m (Kim et al. 2017).

JWST-NIRCam peaks in sensitivity for $\lambda = 3$–5μm, where Zodi is lowest.

Sweet spot for lensing cluster $z \lesssim 0.5$: Zodi-gain mitigates $(1+z)^4$-dimming.

- Minimizes effects from near-IR K-correction and ambient ICL.
- Lower redshift clusters also have higher (virialized) masses and much larger Einstein radii.
- This is critical for optimizing caustic transit detections away from ICL.

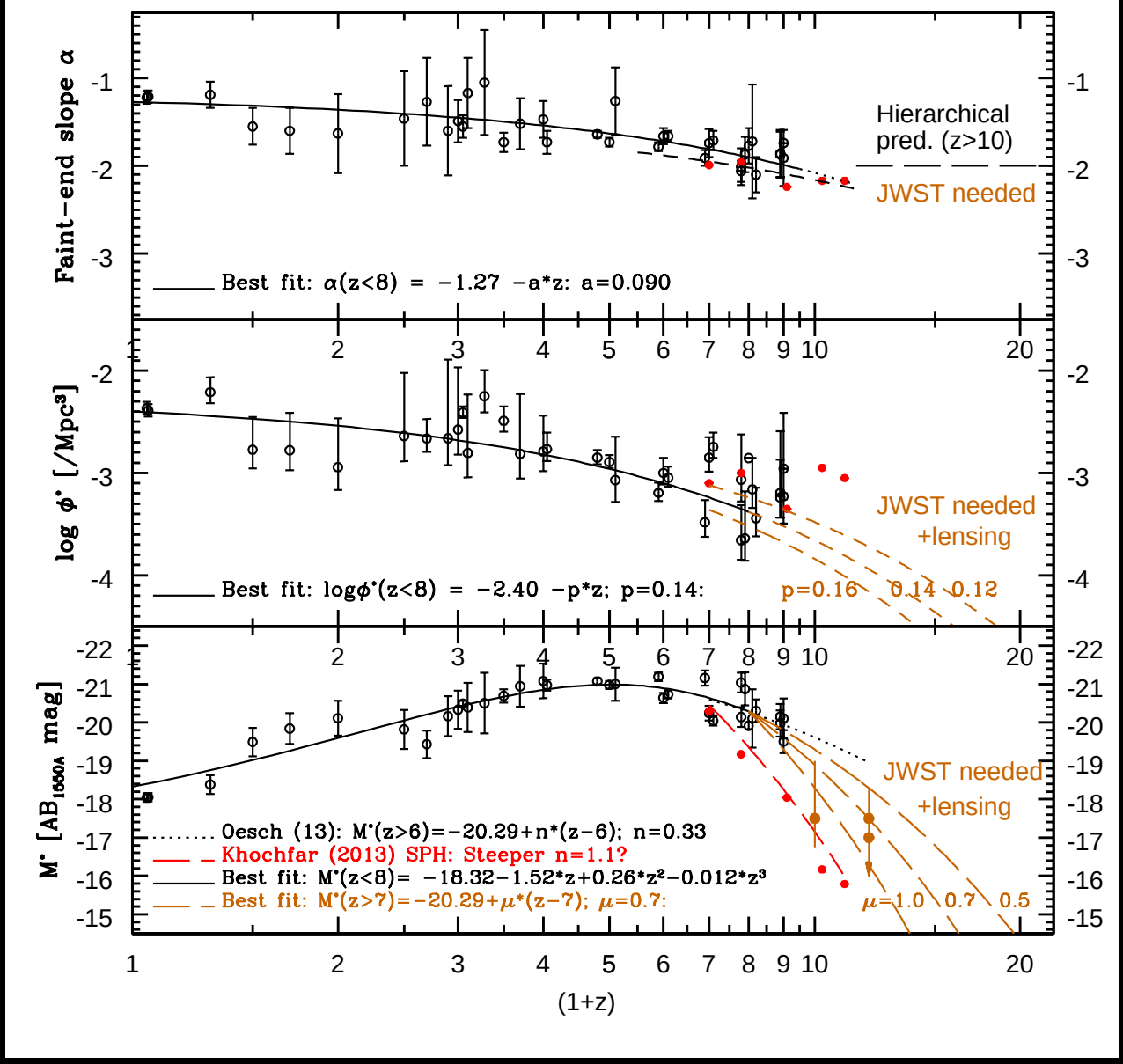

Evolution of Schechter UV-LF: faint-end LF-slope α(z), Φ^* (z) & M^* (z):

- For JWST z$\gtrsim$8, expect $\alpha \lesssim -2.0$; $\Phi^* \lesssim 10^{-3}$ (Mpc$^{-3.5}$) (Oesch$^+$ 11).
- HUDF: Characteristic M^* may drop below –18 or –17.5 mag at z$\gtrsim$10.

$\Rightarrow$ Has significant consequences for JWST survey strategy.

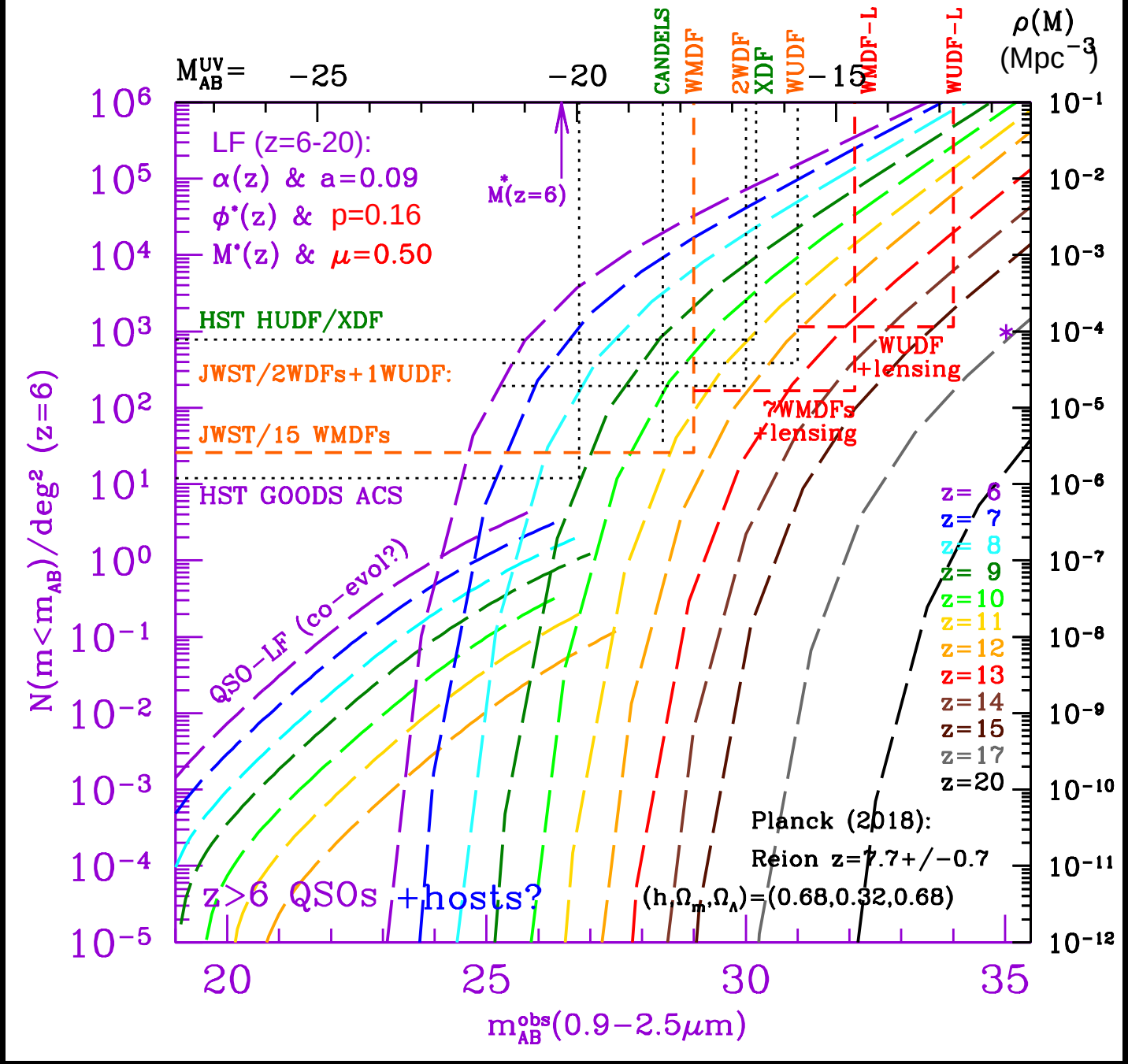

Schechter LF ($z\lesssim6\lesssim20$) with best-fit $\alpha(z)$, Φ^* (z), M^* (z) & μ=0.50.

Area/Sensitivity for: HUDF/XDF, **15 WMDFs**, 2 WDFs, & 1 WUDF.

- Need lensing targets for WMDF–WUDF to see $z\simeq14$–15 objects.

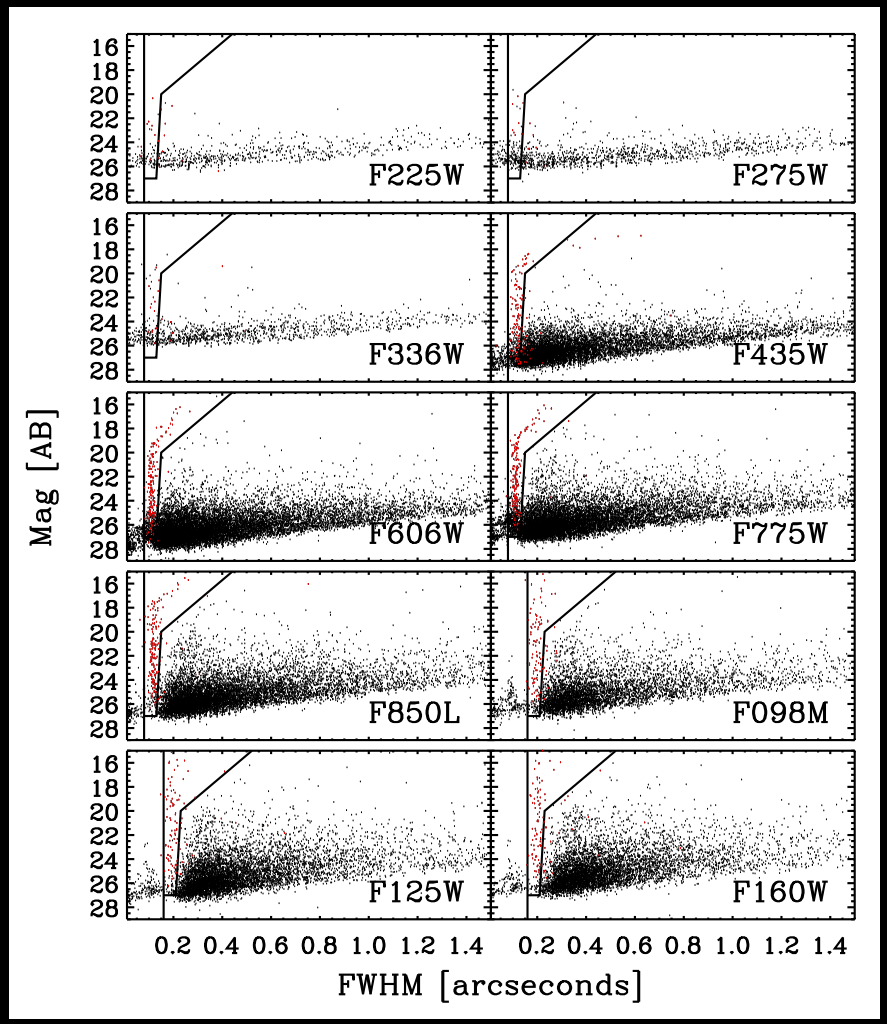

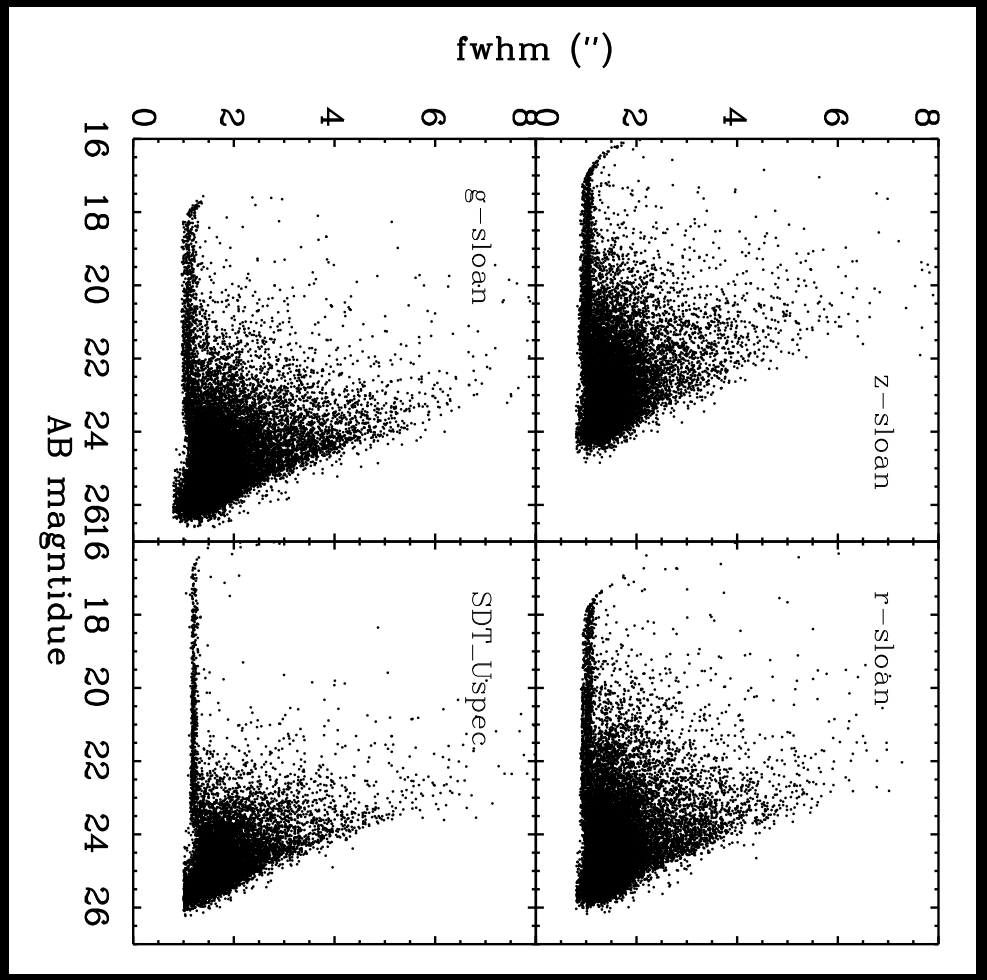

Feasibility of Star-Galaxy Separation in JWST NEP TDF:

[LEFT] 10-filter ERS stars + gals to AB$\lesssim$27 (Windhorst^{+} 2011; W11).

[RIGHT] July 2016 $\boldsymbol{Ugrz}$ LBT/LBC in JWST NEP field to AB$\lesssim$26 mag.

2.5$\times$ smaller drizzled JWST pixels provide very robust star-galaxy separation to AB$\lesssim$29, even in the star-denser NEP field.

(3) JWST Parallax Science possible in the NEP TDF:

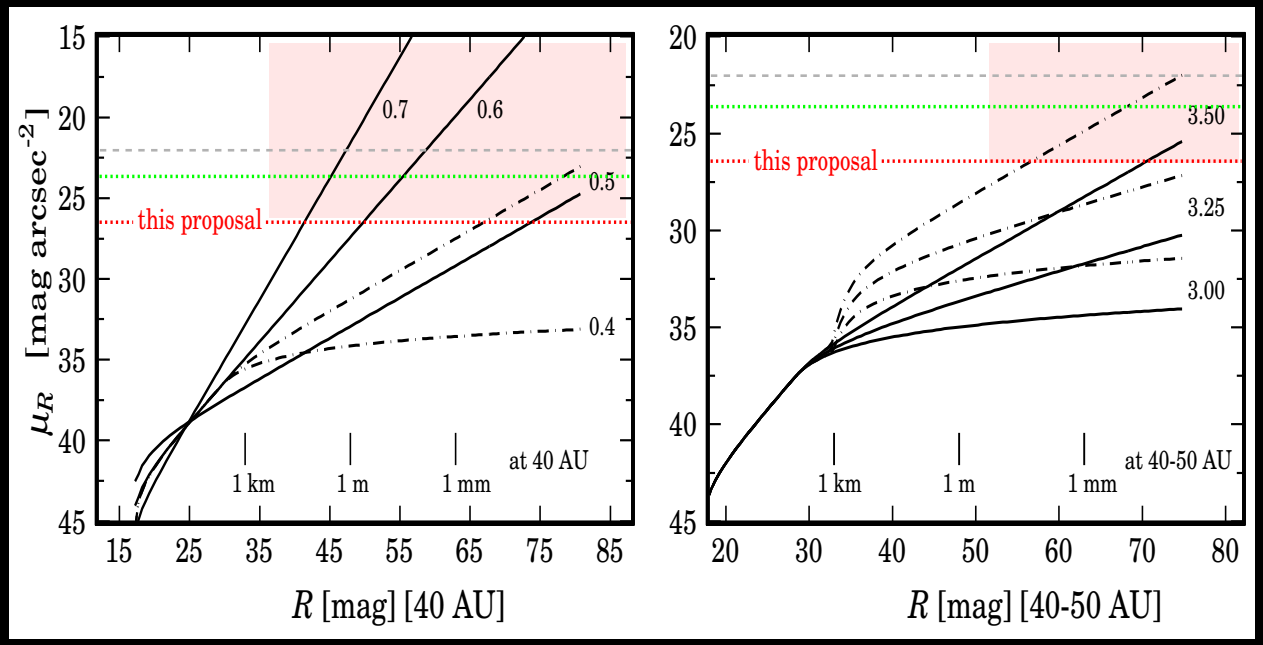

Integrated sky-SB vs. R-mag for KBO's at 40–50 AU (Kenyon & Windhorst 2001).
Models with count-slopes $\alpha \gtrsim 0.55$ (size slopes $\gtrsim D^{-3.5}$) are ruled out.
Tick-marks are KBO-sizes at $\sim$45 AU, assuming Albedo$\sim$0.04.

The JWST NEP TDF will detect & monitor:

- Scattered KBO's/Oort Cloud Objects (OCO's) to AB$\lesssim$29–30 mag.
- KBO's/OCO's with parallaxes $\pi \lesssim 300''$ /yr (distances $\gtrsim$700 AU).
- D$\simeq$3 km diameter objects to 40 AU, D$\simeq$30 km to 400 AU, etc.

- It will require non-standard processing to detect all moving OCO's!

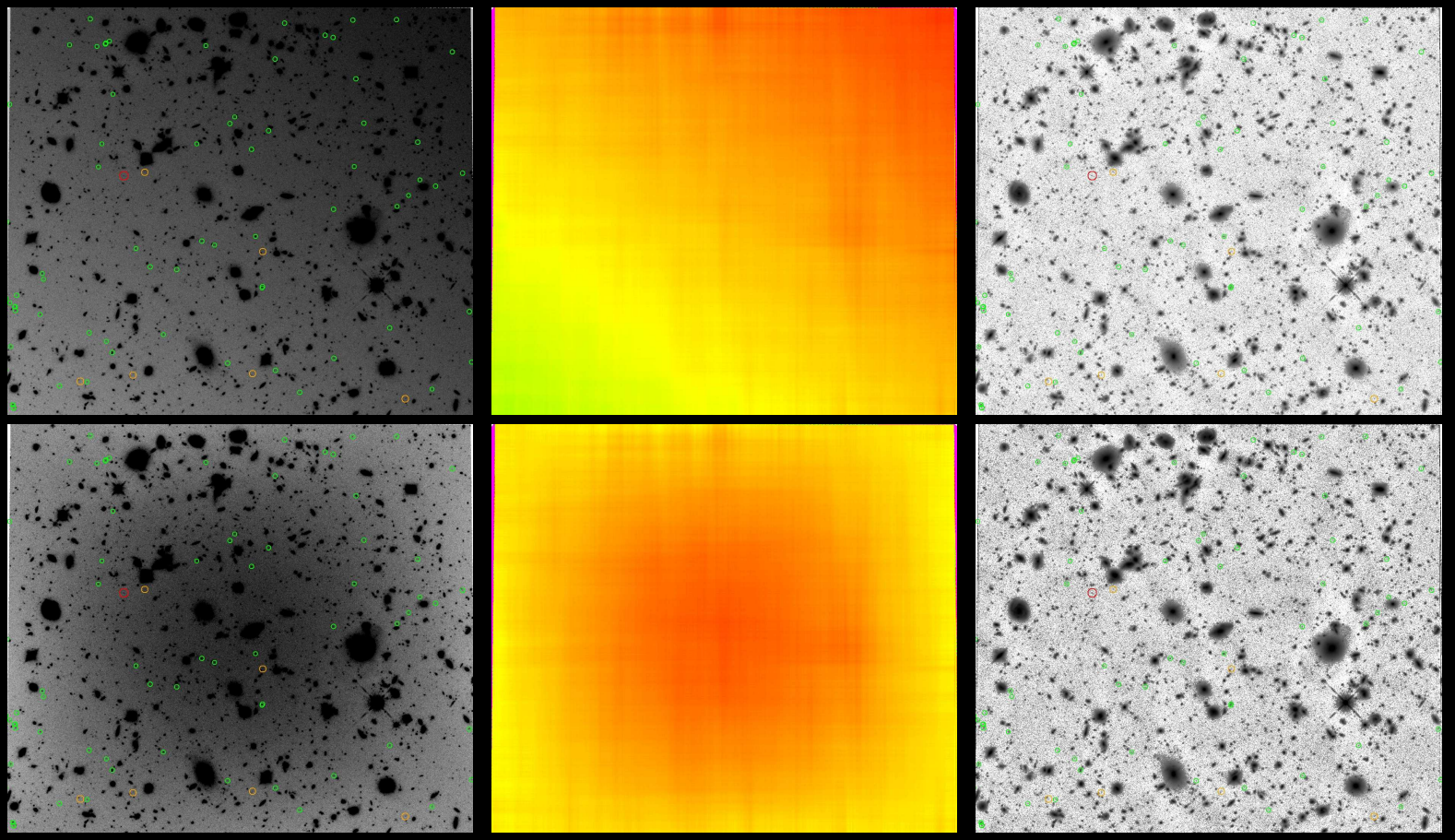

[TOP]: [Left] HUDF F160W image with *worst case* (95% of Zodi) straylight amplitude imposed ± a 4% *linear gradient* from corner-to-corner.

[Middle]: Best fit to sky-background with R. Jansen's "rjbgfit.pro".

[Right]: HUDF image from left with best-fit sky-background subtracted.

[BOTTOM]: Same as top, but with *single-component 2D pattern* superimposed, modeled & removed.

• If JWST straylight has slight or complex gradients, we must carefully plan JWST imaging of lensing clusters with strong ICL.

References and other sources of material shown:

http://www.jwst.nasa.gov/ & http://www.stsci.edu/jwst/

http://ircamera.as.arizona.edu/nircam/

http://www.stsci.edu/jwst/instruments/fgs

Buenzli, E., et al. 2014, Mem. Soc. Astr. It., 85, 690

Gardner, J. P., et al. 2006, Space Science Reviews, 123, 485–606

Jansen, R., & Windhorst, R. 2018, PASP, in press (astro-ph/1807.05278v2)

Kasen, D., Woosley, S.E., & Heger, A. 2011, ApJ 734, 102

Kashlinsky, A., 2016, ApJ, 823, 25

Mather, J., & Stockman, H. 2000, Proc. SPIE Vol. 4013, 2

Rodney, S. A., Riess, A. G., Scolnic, D. M., et al. 2015, AJ, 150, 156

Strolger, L., Dahlen, T., Rodney, S., Graur, O., Riess, A.$^{+}$ 2015, ApJ, 813, 93

Windhorst, R., et al. al., 2011, ApJS, 193, 27 (W11)

Windhorst, R. A., Timmes, F., Wyithe, J. S. B., et al. 2018, ApJS, 234, 41